Relativistic nuclear physics

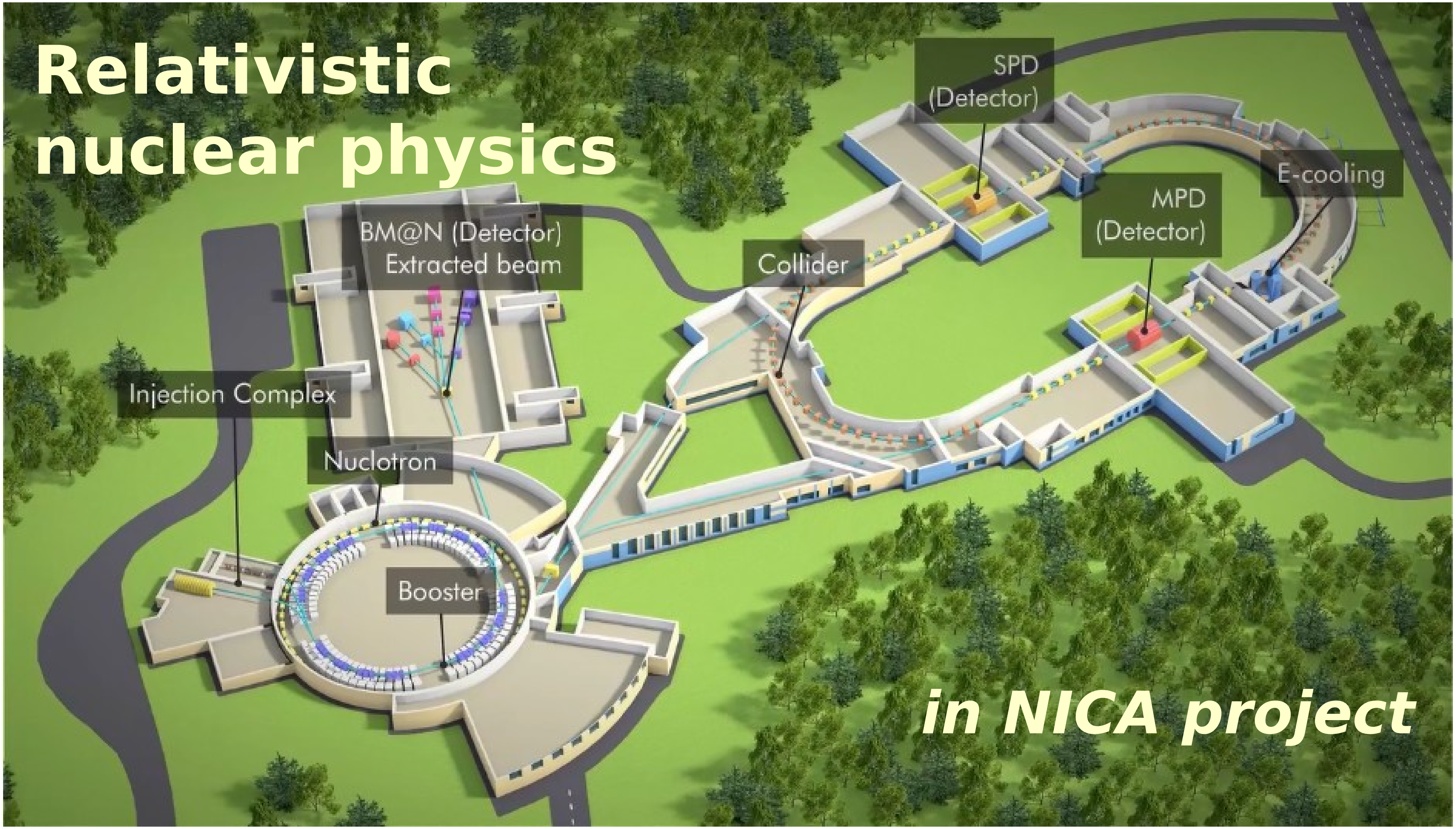

in NICA project

ROGACHEVSKY Oleg
JINR

The Actual Problems
of Microworld Physics
August 28 2023
Minsk

QCD phase diagram

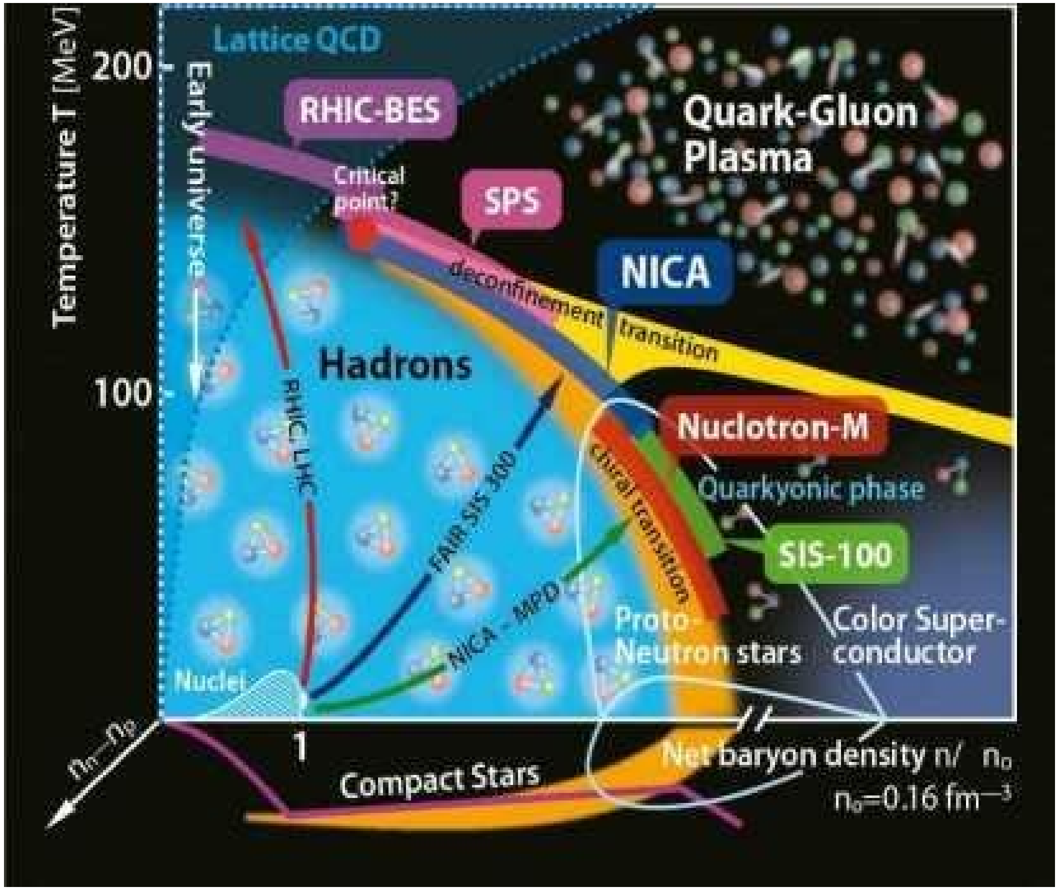

M. Stephanov

XXIV International Symposium on Lattice Field Theory
July 23-28 2006
Tucson Arizona, US
arXiv:hep-lat/0701002v1

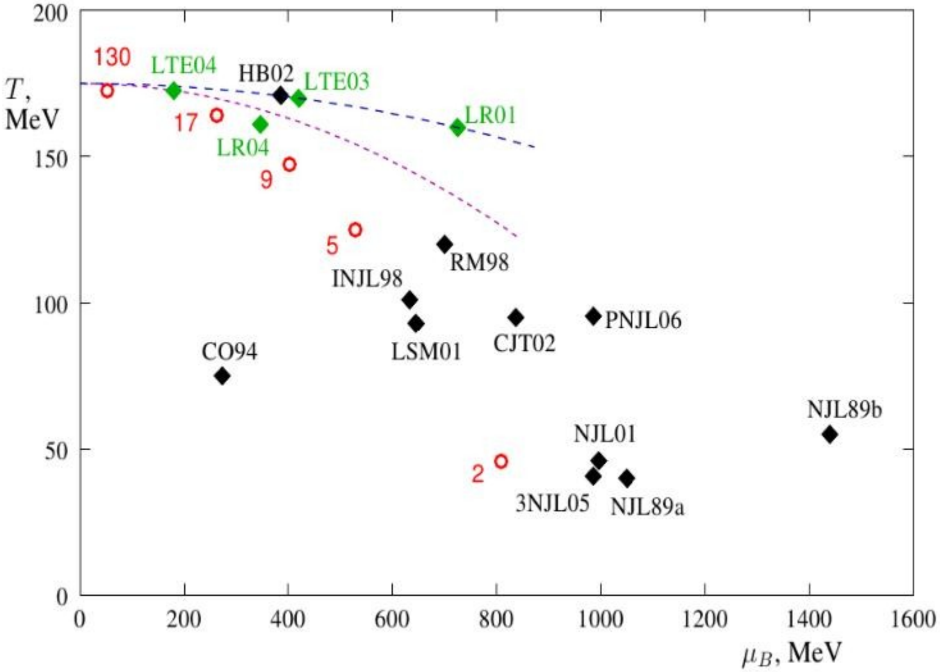

Theoretical predictions

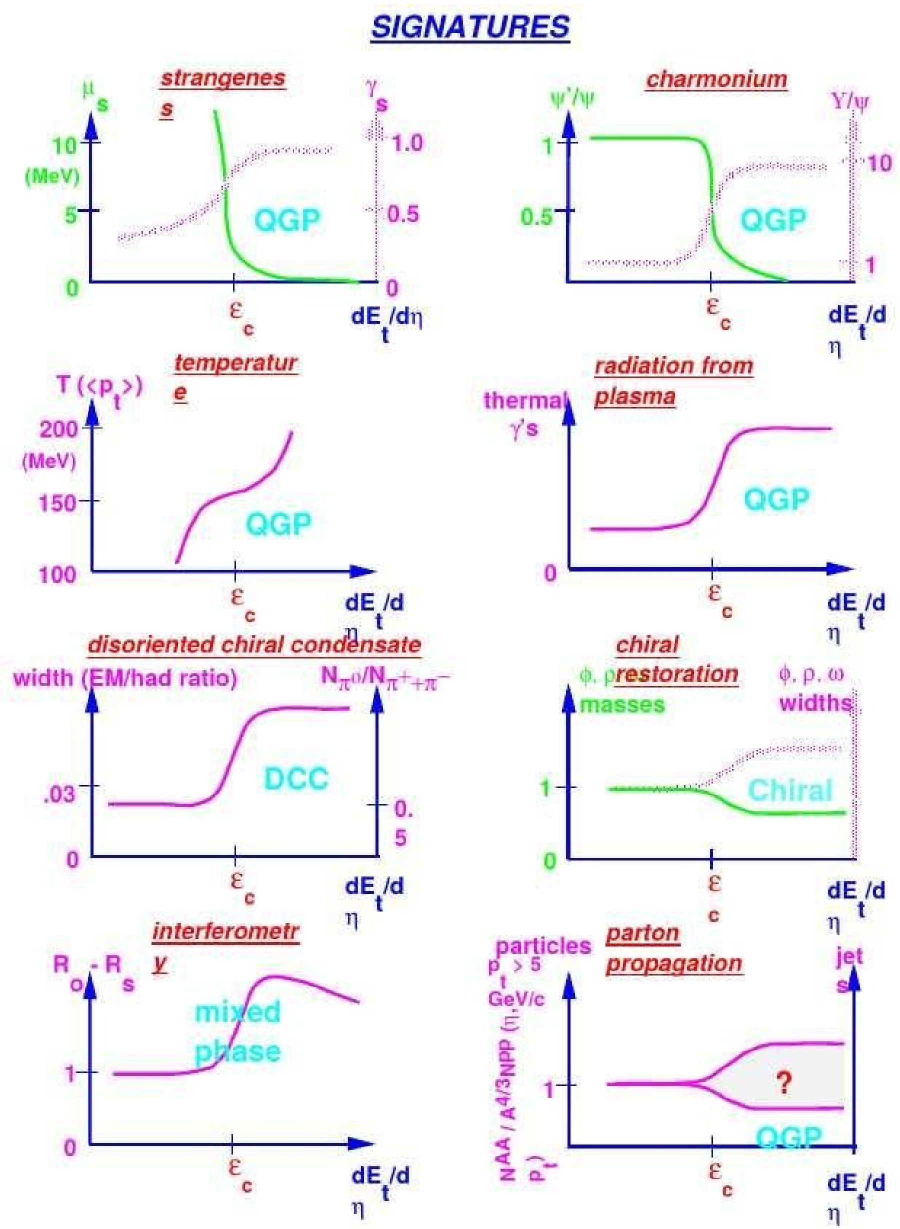

The Search for the Quark-Gluon Plasma

arXiv:hep-ph/9602235

John W. Harris, Berndt Müller

Signatures of quark-gluon plasma formation and the chiral phase transition. The expected behavior of the various signatures is plotted as a function of the measured transverse energy, which is a measure of the energy density, in the region around the critical energy density ε_c of the transition. When two curves are drawn, the hatched curve corresponds to the variable described by the hatched ordinate on the right. See text of review for details

The Quark-Gluon-Plasma is Found at RHIC 2005

BNL -73847-2005
Formal Report

Hunting the Quark Gluon Plasma

RESULTS FROM THE FIRST 3 YEARS AT RHIC

ASSESSMENTS BY THE EXPERIMENTAL COLLABORATIONS

April 18, 2005

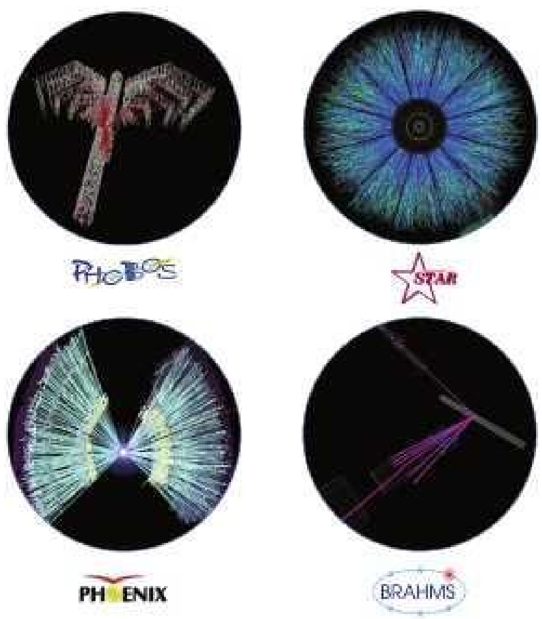

Relativistic Heavy Ion Collider (RHIC) • Brookhaven National Laboratory, Upton, NY 11974-5000

Office of Science U.S. DEPARTMENT OF ENERGY

BROOKHAVEN NATIONAL LABORATORY

CONTENTS

The early measurements have revealed compelling evidence for the existence of a new form of nuclear matter at extremely high density and temperature – a medium in which the predictions of QCD can be tested, and new phenomena explored, under conditions where the relevant degrees of freedom, over nuclear volumes, are expected to be those of quarks and gluons, rather than of hadrons. This is the realm of the quark gluon plasma, the predicted state of matter whose existence and properties are now being explored by the RHIC experiments.

MPD project & mega-project NICA

JOINT INSTITUTE FOR NUCLEAR RESEARCH

Version 1

The MultiPurpose Detector (MPD)
to study Heavy Ion Collisions at NICA

Letter of Intent

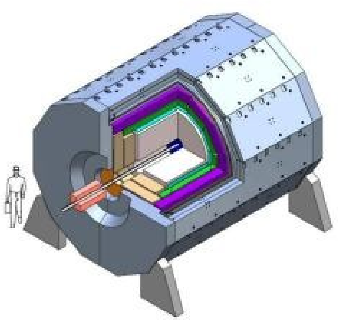

Dubna, 2008

2016

С О Г Л А Ш Е Н И Е

между Правительством Российской Федерации и международной межправительственной научно-исследовательской организацией Объединенным институтом ядерных исследований о создании и эксплуатации комплекса сверхпроводящих колец на встречных пучках тяжелых ионов NICA

Правительство Российской Федерации и международная межправительственная научно-исследовательская организация Объединенный институт ядерных исследований (далее — Объединенный институт ядерных исследований), в дальнейшем именуемые Сторонами,

выражая общее желание содействовать укреплению потенциала Российской Федерации и Объединенного института ядерных исследований в области проводимых научно-технических и инновационных исследований в соответствии со статьей 30 Соглашения между Правительством Российской Федерации и Объединенным институтом ядерных исследований о местопребывании и об условиях деятельности Объединенного института ядерных исследований в Российской Федерации от 23 октября 1995 года,

стремясь создать комплекс сверхпроводящих колец на встречных пучках тяжелых ионов NICA (Nuclotron-based Ion Collider fAcility), обладающий беспрецедентными параметрами в области исследования физики частиц и ядер высоких энергий и обеспечивающий возможность его применения для инновационных разработок в приоритетных областях научных знаний, техники и технологий,

согласились о нижеследующем:

Статья 1

Настоящее Соглашение, заключаемое с целью формирования правовой основы, позволяет Сторонам путем объединения своих материально-технических и финансовых ресурсов вносить вклад в создание и эксплуатацию международного мега-сайенс проекта комплекса сверхпроводящих колец на встречных пучках тяжелых ионов NICA (далее — комплекс NICA), который предусматривает создание ускорительного комплекса для получения пучков тяжелых ионов и

Nuclotron based Ion Collider fAcility

Beams – p,d(h)..$^{197}Au^{79+}$

Collision energy $\sqrt{s}$= **4-11** GeV/u (Au), **12-27** (p)

Beam energy (fixed target) - **1-6** GeV/u

Luminosity: 1**0**^{27} cm^{-2}s^{-1}(Au), **10**^{32} (p)

Experiments:

2 Interaction points – **MPD** and SPD

Fixed target experiment **BM@N**

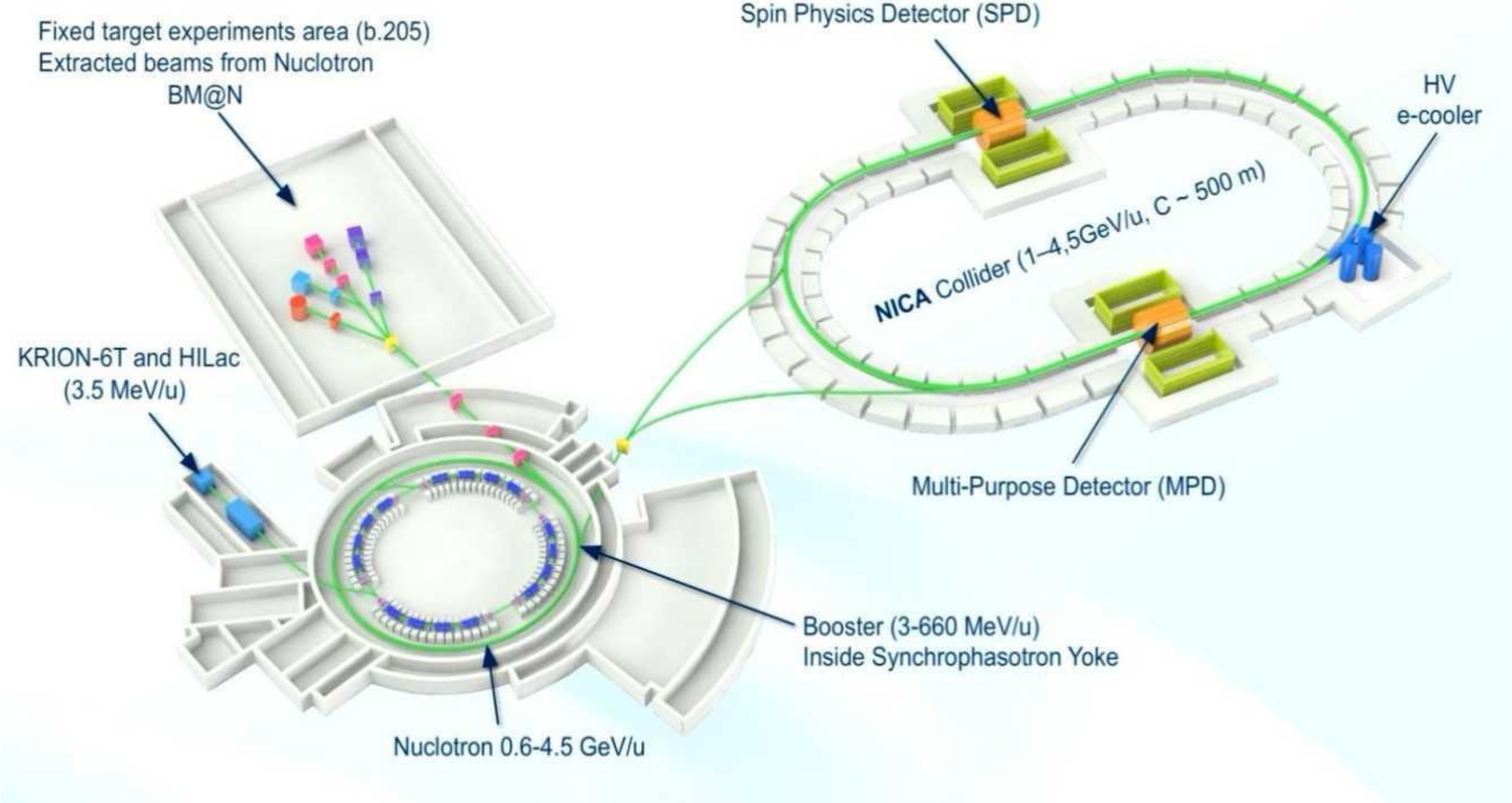

NICA advantagies

J. Cleymans
MPD collaboration Meeting April, 2018

- ✔ Maximum in K^+/π^+ ratio is in the NICA energy region,
- ✔ Maximum in Λ/π ratio is in the NICA energy region,
- ✔ Maximum in the net baryon density is in the NICA energy region,
- ✔ Transition from a baryon dominated system to a meson dominated one happens in the NICA energy region.

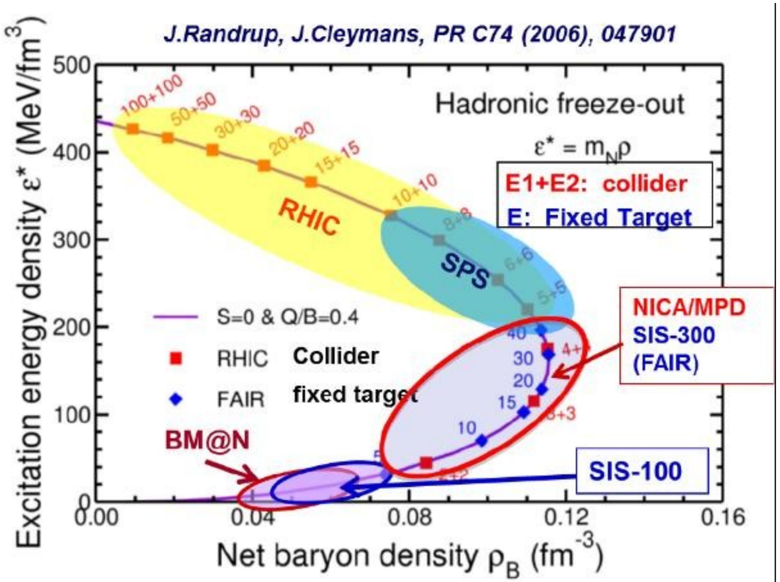

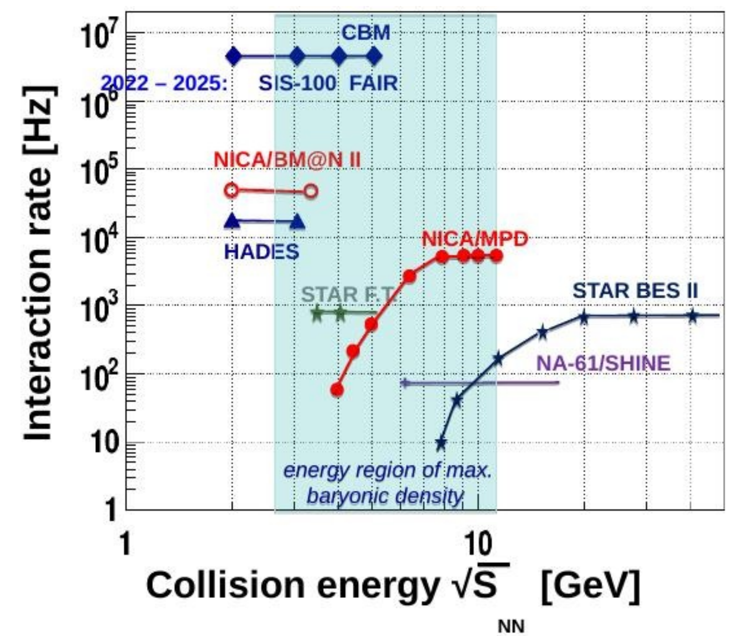

Studying the Phase Diagram of QCD Matter at RHIC

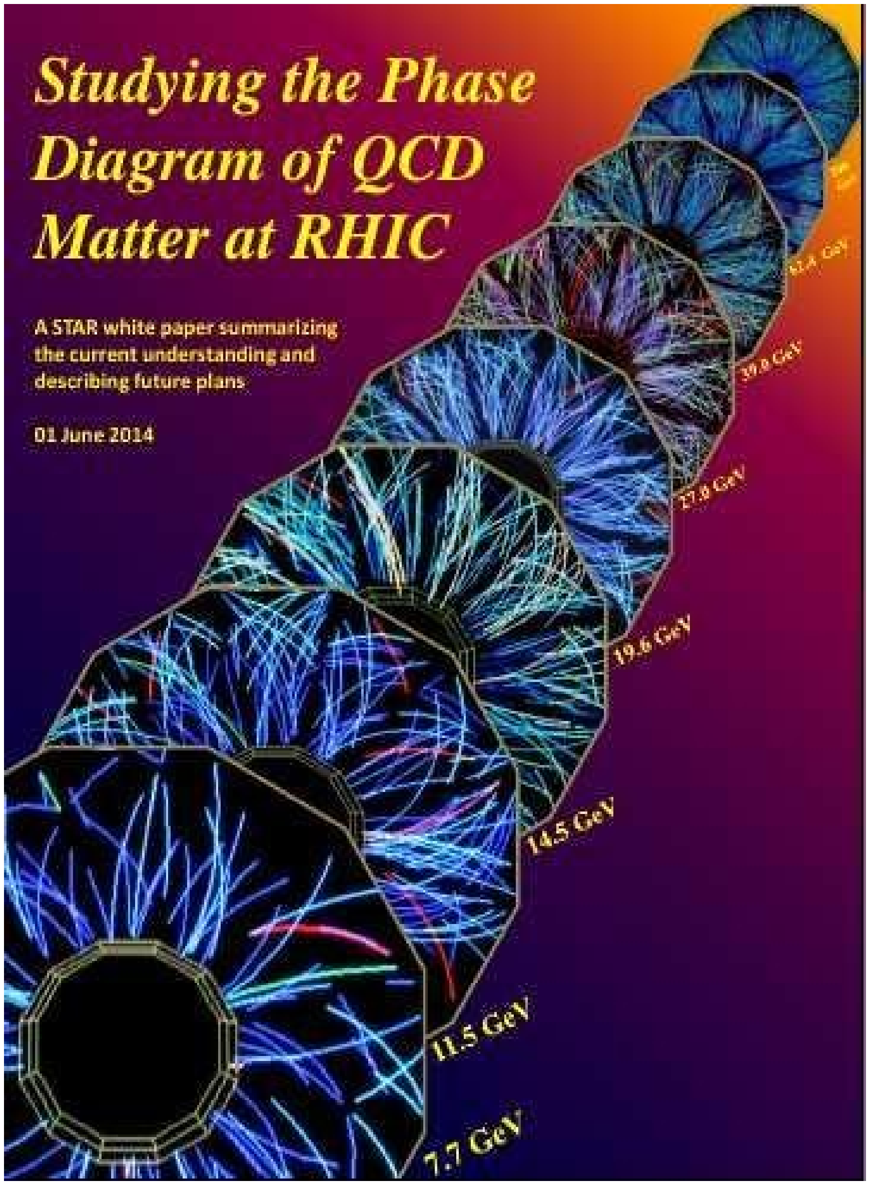

Contents

STAR BES QGP signatures

The particular observables that STAR has identified as the essential drivers of our run plan are:

(A-1) Constituent-quark-number scaling of v_2 , indicating partonic degrees of freedom;
(A-2) Hadron suppression in central collisions as characterized by the ratio R_{CP} ;
(A-3) Untriggered pair correlations in the space of pair separation in azimuth and pseudorapidity, which elucidate the ridge phenomenon;
(A-4) Local parity violation in strong interactions, an emerging and important RHIC discovery in its own right, is generally believed to require deconfinement, and thus also is expected to turn-off at lower energies.

A search for signatures of a phase transition and a critical point. The particular observables that we have identified as the essential drivers of our run plan are:

(B-1) Elliptic & directed flow for charged particles and for identified protons and pions, which have been identified by many theorists as highly promising indicators of a "softest point" in the nuclear equation of state;
(B-2) Azimuthally-sensitive femtoscopy, which adds to the standard HBT observables by allowing the tilt angle of the ellipsoid-like particle source in coordinate space to be measured; these measurements hold promise for identifying a softest point, and complements the momentum-space information revealed by flow measurements, and
(B-3) Fluctuation measures, indicated by large jumps in the baryon, charge and strangeness susceptibilities, as a function of system temperature – the most obvious expected manifestation of critical phenomena.

RHIC BES II program

Run	species	total particle energy [GeV/nucleon]	calendar time in physics	total delivered luminosity	average store polarization, (H-jet)[a]
Run-18 CY2017/18, FY2018 28.0 cryo-weeks	$^{96}\mathrm{Zr}^{40+} + {}^{96}\mathrm{Zr}^{40+}$	100.0	28.5 days	3.9 nb^{-1}	—
	$^{96}\mathrm{Ru}^{44+} + {}^{96}\mathrm{Ru}^{44+}$	100.0	28.5 days	4.00 nb^{-1}	—
	$^{197}\mathrm{Au}^{79+} + {}^{197}\mathrm{Au}^{79+}$	13.5	24.0 days	282 $\mu\mathrm{b}^{-1}$	—
	$^{197}\mathrm{Au}^{79+}$ + fixed target $^{197}\mathrm{Au}$	3.85	4.6 days	63 $\mu\mathrm{b}^{-1}$	—
	$^{197}\mathrm{Au}^{79+}$ + fixed target $^{197}\mathrm{Au}$	26.5	7.7 days	33 $\mu\mathrm{b}^{-1}$	—
Run-19 CY2018/19, FY2019 28.0 cryo-weeks	$^{197}\mathrm{Au}^{79+} + {}^{197}\mathrm{Au}^{79+}$	9.8	36 days	151 $\mu\mathrm{b}^{-1}$	—
	$^{197}\mathrm{Au}^{79+} + {}^{197}\mathrm{Au}^{79+}$	7.3	60 days	132 $\mu\mathrm{b}^{-1}$	—
	$^{197}\mathrm{Au}^{79+}$ + fixed target $^{197}\mathrm{Au}$	7.3	11 hours	11 $\mu\mathrm{b}^{-1}$	—
	$^{197}\mathrm{Au}^{79+} + {}^{197}\mathrm{Au}^{79+}$	3.85	24 days	3.6 $\mu\mathrm{b}^{-1}$	—
	$^{197}\mathrm{Au}^{79+}$ + fixed target $^{197}\mathrm{Au}$	3.85	2 hours	1.1 $\mu\mathrm{b}^{-1}$	—
	$^{197}\mathrm{Au}^{79+}$ + fixed target $^{197}\mathrm{Au}$	4.59	2 days	42 $\mu\mathrm{b}^{-1}$	—
	$^{197}\mathrm{Au}^{79+} + {}^{197}\mathrm{Au}^{79+}$	4.59	6 days	7.0 $\mu\mathrm{b}^{-1}$	—
	$^{197}\mathrm{Au}^{79+}$ + fixed target $^{197}\mathrm{Au}$	31.2	13 hours	11 $\mu\mathrm{b}^{-1}$	—
	$^{197}\mathrm{Au}^{79+} + {}^{197}\mathrm{Au}^{79+}$	100.0	1.5 days	80 $\mu\mathrm{b}^{-1}$	—
Run-20 CY2019/20, FY2020 28.0 cryo-weeks +12.4 weeks with cold machine but no operation due to COVID-19	$^{197}\mathrm{Au}^{79+} + {}^{197}\mathrm{Au}^{79+}$	5.75	62 days	143 $\mu\mathrm{b}^{-1}$	—
	$^{197}\mathrm{Au}^{79+} + {}^{197}\mathrm{Au}^{79+}$	4.59	117 days	176 $\mu\mathrm{b}^{-1}$	—
	$^{197}\mathrm{Au}^{79+}$ + fixed target $^{197}\mathrm{Au}$	31.2	1.1 days	23 $\mu\mathrm{b}^{-1}$	—
	$^{197}\mathrm{Au}^{79+}$ + fixed target $^{197}\mathrm{Au}$	19.5	1.4 days	23 $\mu\mathrm{b}^{-1}$	—
	$^{197}\mathrm{Au}^{79+}$ + fixed target $^{197}\mathrm{Au}$	13.5	1.0 days	25 $\mu\mathrm{b}^{-1}$	—
	$^{197}\mathrm{Au}^{79+}$ + fixed target $^{197}\mathrm{Au}$	9.8	0.9 days	21 $\mu\mathrm{b}^{-1}$	—
	$^{197}\mathrm{Au}^{79+}$ + fixed target $^{197}\mathrm{Au}$	7.3	1.1 days	24 $\mu\mathrm{b}^{-1}$	—
	$^{197}\mathrm{Au}^{79+}$ + fixed target $^{197}\mathrm{Au}$	5.75	0.9 days	24 $\mu\mathrm{b}^{-1}$	—
	$^{197}\mathrm{Au}^{79+}$ + fixed target $^{197}\mathrm{Au}$	26.5	1.9 days	65 $\mu\mathrm{b}^{-1}$	—
Run-21 CY2020/21, FY2021 24.0 cryo-weeks	$^{197}\mathrm{Au}^{79+} + {}^{197}\mathrm{Au}^{79+}$	3.85	12.1 weeks	152 $\mu\mathrm{b}^{-1}$	—
	$^{197}\mathrm{Au}^{79+}$ + fixed target $^{197}\mathrm{Au}$	3.85	22 days	431 $\mu\mathrm{b}^{-1}$	—
	$^{197}\mathrm{Au}^{79+}$ + fixed target $^{197}\mathrm{Au}$	44.5	1 day	10 $\mu\mathrm{b}^{-1}$	—
	$^{197}\mathrm{Au}^{79+}$ + fixed target $^{197}\mathrm{Au}$	70	1 day	10 $\mu\mathrm{b}^{-1}$	—
	$^{197}\mathrm{Au}^{79+}$ + fixed target $^{197}\mathrm{Au}$	100	1 day	11 $\mu\mathrm{b}^{-1}$	—
	$^{16}\mathrm{O}^{8+} + {}^{16}\mathrm{O}^{8+}$	100	14 days	32 nb^{-1}	—
	$^{197}\mathrm{Au}^{79+} + {}^{197}\mathrm{Au}^{79+}$	8.65	11 days	83 $\mu\mathrm{b}^{-1}$	—
	$^{197}\mathrm{Au}^{79+}$ + fixed target $^{197}\mathrm{Au}$	26.5	1 day	18 $\mu\mathrm{b}^{-1}$	—
	d + $^{197}\mathrm{Au}^{79+}$	100.7 + 100.0	4 days	1.25 nb^{-1}	—
Run-22 CY2021/22, FY2022 20.0 cryo-weeks	polarized p + p	254.2	16.9 weeks	807 pb^{-1}	50%
Run-23 CY2022/23, FY2023 5.0+20.0 cryo-weeks (planned)	$^{197}\mathrm{Au}^{79+} + {}^{197}\mathrm{Au}^{79+}$	100.0	10.6 weeks	5.7 nb^{-1}	—

STAR data BES II program

$\sqrt{s_{NN}}$ (GeV)	Beam Energy (GeV/nucleon)	Collider or Fixed Target	$y_{center\ of\ mass}$	μ_B (MeV)	Run Time (days)	No. Events Collected (Request)	Date Collected
200	100	C	0	25	2.0	138 M (140 M)	Run-19
27	13.5	C	0	156	24	555 M (700 M)	Run-18
19.6	9.8	C	0	206	36	582 M (400 M)	Run-19
17.3	8.65	C	0	230	14	256 M (250 M)	Run-21
14.6	7.3	C	0	262	60	324 M (310 M)	Run-19
13.7	100	FXT	2.69	276	0.5	52 M (50 M)	Run-21
11.5	5.75	C	0	316	54	235 M (230 M)	Run-20
11.5	70	FXT	2.51	316	0.5	50 M (50 M)	Run-21
9.2	4.59	C	0	372	102	162 M (160 M)	Run-20+20b
9.2	44.5	FXT	2.28	372	0.5	50 M (50 M)	Run-21
7.7	3.85	C	0	420	90	100 M (100 M)	Run-21
7.7	31.2	FXT	2.10	420	0.5+1.0+ scattered	50 M + 112 M + 100 M (100 M)	Run-19+20+21
7.2	26.5	FXT	2.02	443	2+Parasitic with CEC	155 M + 317 M	Run-18+20
6.2	19.5	FXT	1.87	487	1.4	118 M (100 M)	Run-20
5.2	13.5	FXT	1.68	541	1.0	103 M (100 M)	Run-20
4.5	9.8	FXT	1.52	589	0.9	108 M (100 M)	Run-20
3.9	7.3	FXT	1.37	633	1.1	117 M (100 M)	Run-20
3.5	5.75	FXT	1.25	666	0.9	116 M (100 M)	Run-20
3.2	4.59	FXT	1.13	699	2.0	200 M (200 M)	Run-19
3.0	3.85	FXT	1.05	721	4.6	259 M -> 2B(100 M -> 2B)	Run-18+21

STAR publications for BES II

- First Observation of Directed Flow of Hypernuclei H3L and H4L in sqrt(sNN) = 3 GeV Au+Au Collisions at RHIC
  Phys. Rev. Lett. 130 (2023) 212301
- Higher-order cumulants and correlation functions of proton multiplicity distributions in sqrt{sNN} = 3 GeV Au + Au collisions at the RHIC STAR experiment
  Phys. Rev. C 107 (2023) 24908
- Probing Strangeness Canonical Ensemble with K-, phi(1020) and Xi- Production in Au+Au Collisions at sqrt{s_NN} = 3 GeV
  Phys. Lett. B 831 (2022) 137152
- Light Nuclei Collectivity from 3 GeV Au+Au Collisions at RHIC
  Phys. Lett. B 827 (2022) 136941
- Measurements of Proton High Order Cumulants in sqrt{s_NN} = 3 GeV Au+Au Collisions and Implications for the QCD Critical Point
  Phys. Rev. Lett. 128 (2022) 202303
- Disappearance of partonic collectivity in 3 GeV Au+Au collisions at RHIC
  Phys. Lett. B 827 (2022) 137003

STAR publication at 7.7 GeV

- K0 production in Au+Au collisions at sqrt{sNN} = 7.7, 11.5, 14.5, 19.6, 27 and 39 GeV from RHIC beam energy scan
  Phys. Rev. C 107 (2023) 34907

- Strange hadron production in Au+Au collisions at sqrt(sNN) = 7.7, 11.5, 19.6, 27, and 39 GeV
  Phys. Rev. C 102 (2020) 34909

- Measurement of elliptic flow of light nuclei at sqrt(sNN)= 200, 62.4, 39, 27, 19.6, 11.5, and 7.7 GeV at RHIC
  Phys. Rev. C 94 (2016) 34908

- Centrality dependence of identified particle elliptic flow in relativistic heavy ion collisions at sqrt(sNN)= 7.7-62.4 GeV
  Phys. Rev. C 93 (2016) 14907

- Energy Dependence of K-pi, p-pi, and K-p Fluctuations in Au+Au Collisions from sqrt(sNN) = 7.7 to 200 GeV
  Phys. Rev. C 92 (2015) 21901

- Elliptic flow of identified hadrons in Au+Au collisions at $\sqrt{s_{NN}}=$ 7.7--62.4 GeV
  Phys. Rev. C 88 (2013) 14902

- Inclusive charged hadron elliptic flow in Au + Au collisions at $\sqrt{s_{NN}}$ = 7.7 - 39 GeV
  Phys. Rev. C 86 (2012) 54908

STAR publication at 11.5 GeV

- K0 production in Au+Au collisions at sqrt{sNN} = 7.7, 11.5, 14.5, 19.6, 27 and 39 GeV from RHIC beam energy scan

  Phys. Rev. C 107 (2023) 34907

- Strange hadron production in Au+Au collisions at sqrt(sNN) = 7.7, 11.5, 19.6, 27, and 39 GeV

  Phys. Rev. C 102 (2020) 34909

- Beam Energy Dependence of Jet-Quenching Effects in Au+Au Collisions at sqrt(sNN) = 7.7, 11.5, 14.5, 19.6, 27, 39, and 62.4 GeV

  Phys. Rev. Lett. 121 (2018) 32301

- Measurement of elliptic flow of light nuclei at sqrt(sNN)= 200, 62.4, 39, 27, 19.6, 11.5, and 7.7 GeV at RHIC

  Phys. Rev. C 94 (2016) 34908

STAR BES II studies

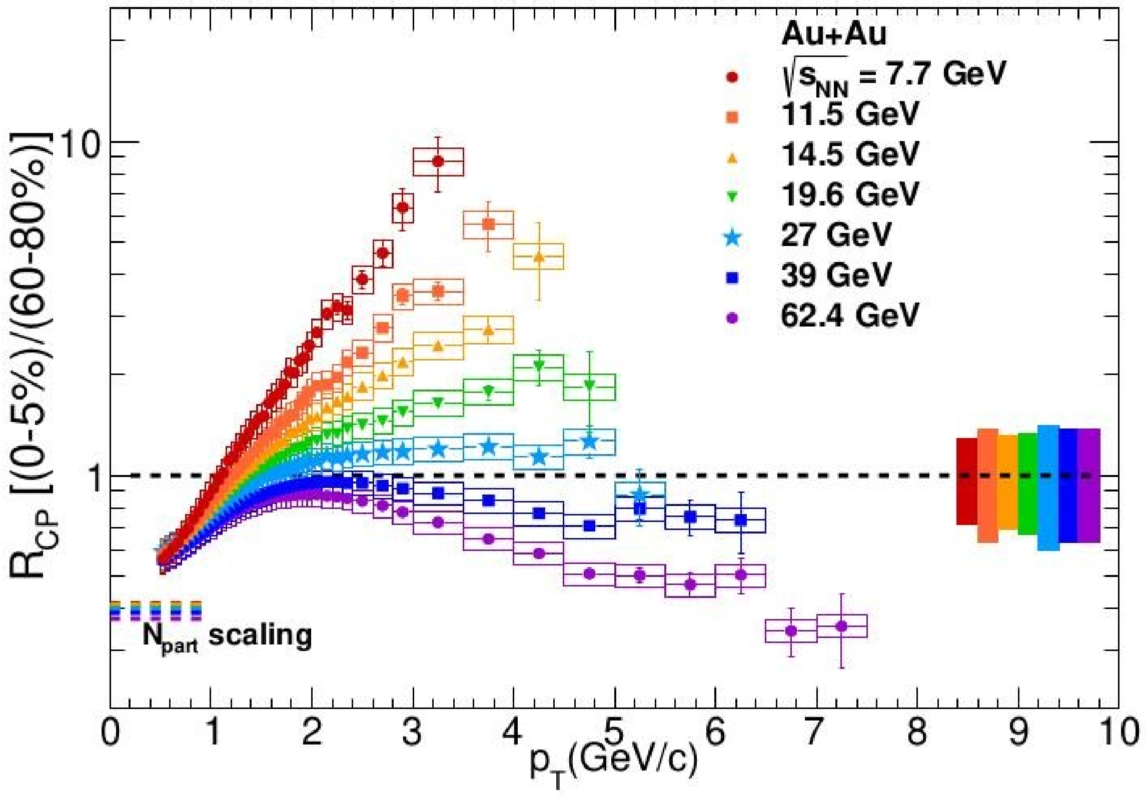

Charged hadron R_{CP} for RHIC BES energies. The uncertainty bands at unity on the right side of the plot correspond to the p_T independent uncertainty in N coll scaling with the color in the band corresponding to the color of the data points for that energy. The vertical uncertainty bars correspond to statistical uncertainties and the boxes to systematic uncertainties.

Phys. Rev. C 102 (2020) 34909

Phys. Rev. Lett. 121 (2018) 32301

STAR BES II studies

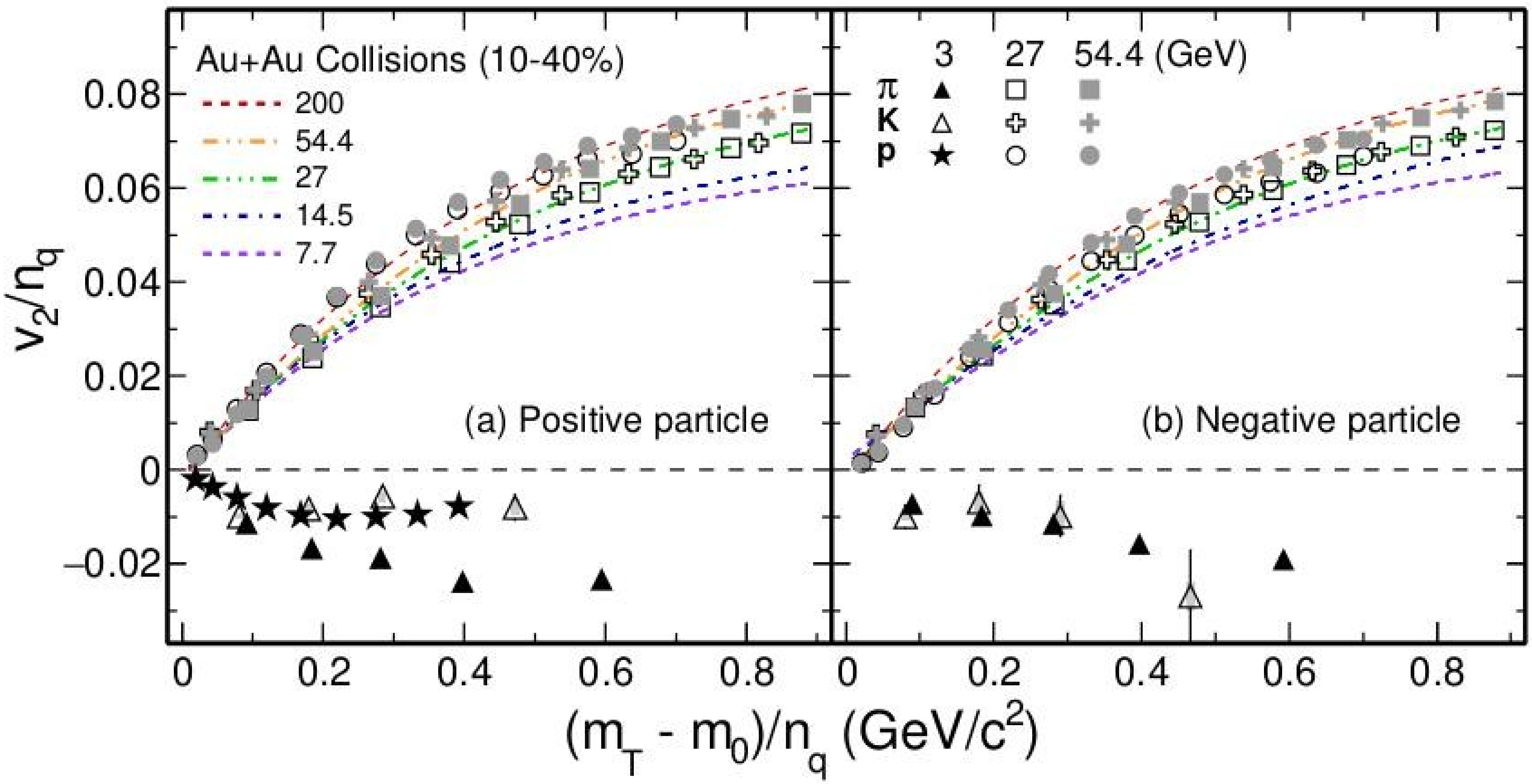

v_2 scaled by the number of constituent quarks, v_2/n_q, as a function of scaled transverse kinetic energy for pions, kaons and protons from Au+Au collisions in 10-40% centrality at $\sqrt{s_{NN}}$ = 3, 27, and 54.4 GeV for positive charged particles and negative charged particles (right panel). The measurements are in the rapidity range $|y| < 0.5$ at 27 and 54.4 GeV, and in $-0.5 < y < 0$ at 3 GeV. Colored dashed lines represent the scaling fit to data from Au+Au collisions at 7.7, 14.5, 27, 54.4, and 200 GeV from STAR experiment at RHIC.

NICA White Paper

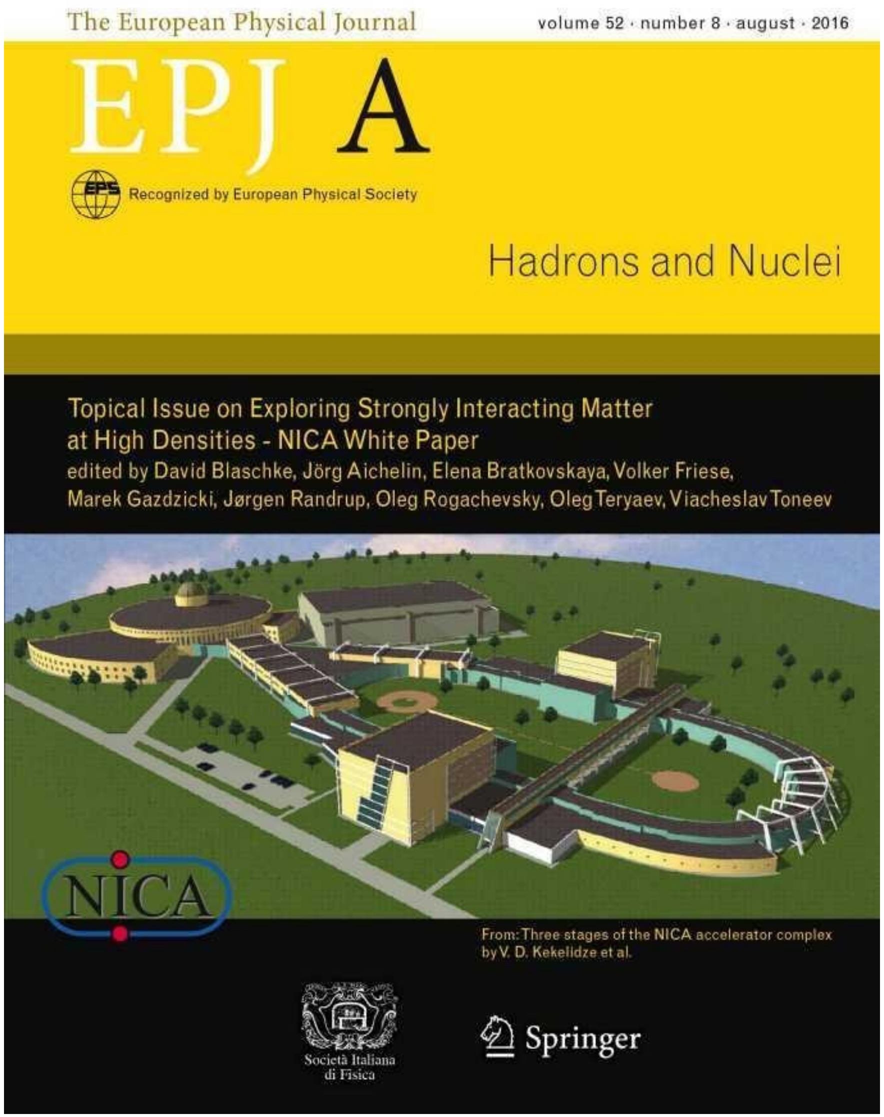

ФИЗИКА ЭЛЕМЕНТАРНЫХ ЧАСТИЦ И АТОМНОГО ЯДРА
2016. Т. 47. ВЫП. 4

FEASIBILITY STUDY OF HEAVY ION PHYSICS PROGRAM AT NICA

P. N. Batyuk [1,*], *V. D. Kekelidze* [1], *V. I. Kolesnikov* [1],
O. V. Rogachevsky [1], *A. S. Sorin* [1,2], *V. V. Voronyuk* [1]
on behalf of the BM@N and MPD collaborations

[1] Joint Institute for Nuclear Research, Dubna
[2] National Research Nuclear University
"Moscow Engineering Physics Institute" (MEPhI), Moscow

There is strong experimental and theoretical evidence that in collisions of heavy ions at relativistic energies the nuclear matter undergoes a phase transition to the deconfined state — Quark–Gluon Plasma. The caused energy region of such a transition was not found at high energy at SPS and RHIC, and search for this energy is shifted to lower energies, which will be covered by the future NICA (Dubna), FAIR (Darmstadt) facilities and BES II at RHIC. Fixed target and collider experiments at the NICA facility will work in the energy range from a few A GeV up to $\sqrt{s_{NN}} = 11$ GeV and will study the most interesting area on the nuclear matter phase diagram.

The most remarkable results were observed in the study of collective phenomena occurring in the early stage of nuclear collisions. Investigation of the collective flow will provide information on Equation of State (EoS) for nuclear matter. Study of the event-by-event fluctuations and correlations can give us signals of critical behavior of the system. Femtoscopy analysis provides the space-time history of the collisions. Also, it was found that baryon stopping power revealing itself as a "wiggle" in the excitation function of curvature of the (net) proton rapidity spectrum relates to the order of the phase transition.

The available observations of an enhancement of dilepton rates at low invariant masses may serve as a signal of the chiral symmetry restoration in hot and dense matter. Due to this fact, measurements of the dilepton spectra are considered to be an important part of the NICA physics program. The study of strange particles and hypernuclei production gives additional information on the EoS and "strange" axis of the QCD phase diagram.

In this paper a feasibility of the considered investigations is shown by the detailed Monte Carlo simulations applied to the planned experiments (BM@N, MPD) at NICA.

NICA 2018: collaborations

33 institutes   > 450 participants

10 institutes   ~ 189 participants

30 institutes

MPD experiment at NICA

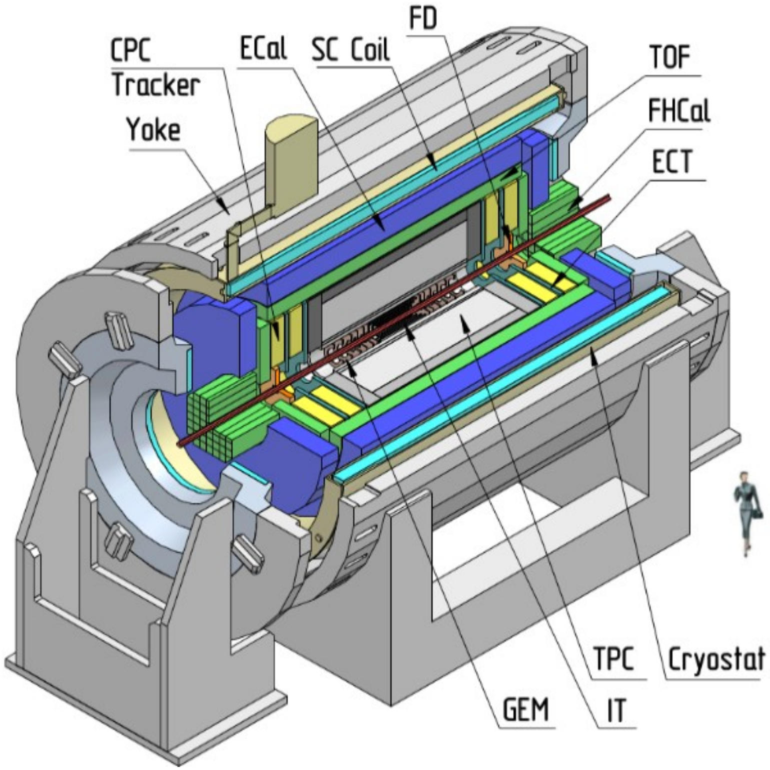

MPD eventdisplay
AuAu √s = 11 GeV

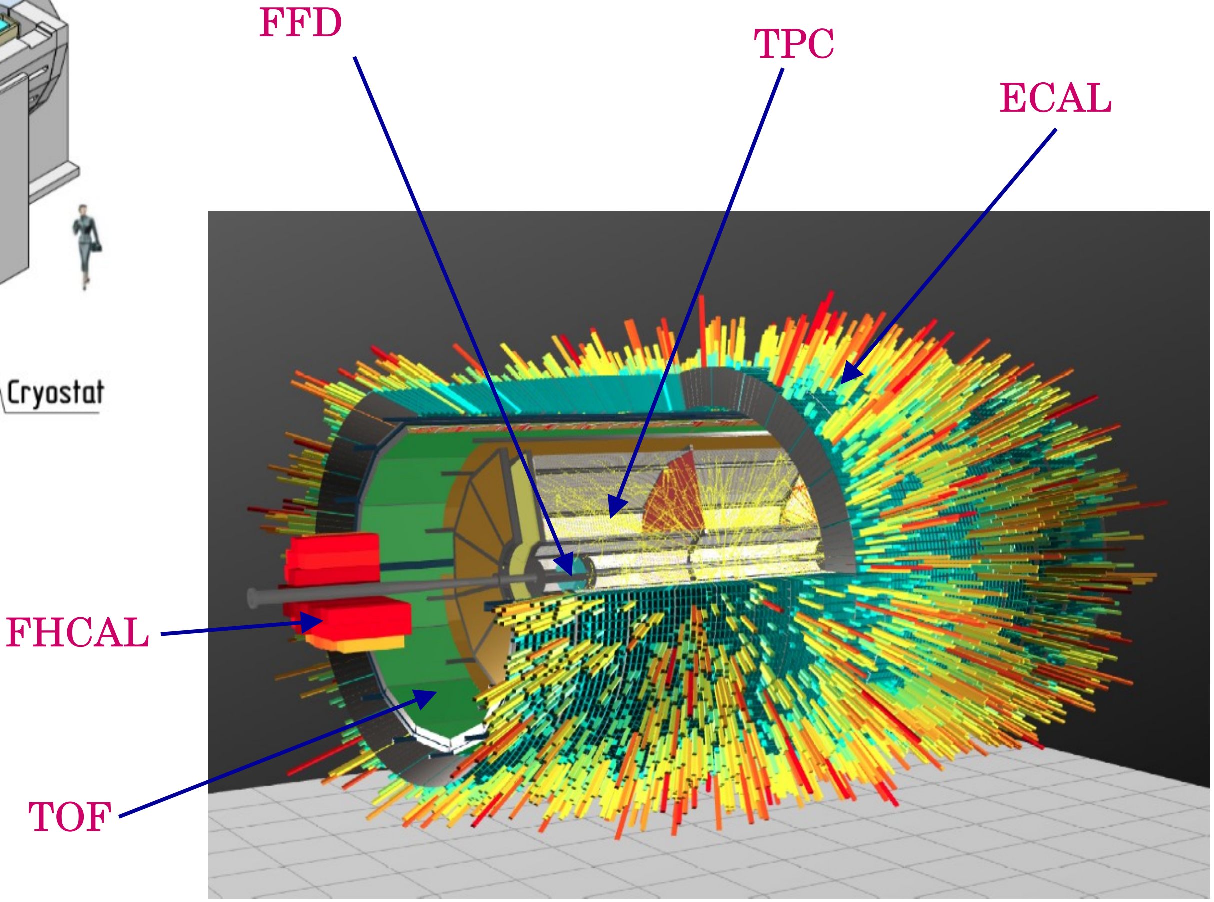

MPD experiment 1-st stage

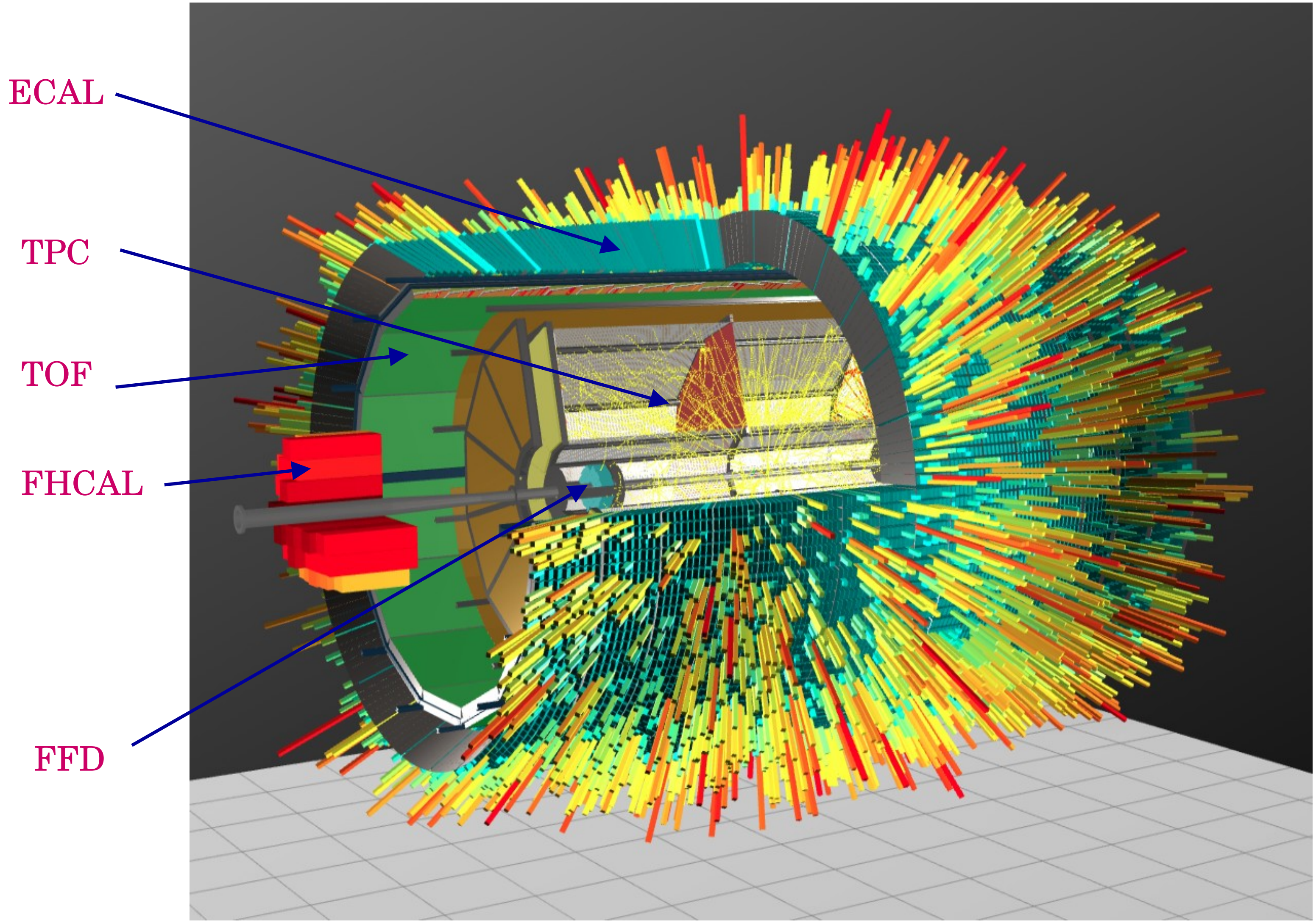

MPD data mass production

Generator	PWG	Coll.		# of events() 10^6	Reco
UrQMD	PWG4	AuAu	11	15	+
		BiBi	9	10	+
			9.46	10	+
			9.2	95	+
	PWG2	AuAu	11	10	+
	PWG3	AuAu	7.7	10	+
		BiBi	7.7	10	+
			9	15	+
		pp	9	10	+
	PWG1	BiBi	9.2	11(50 underway)	+
DCM-SMM	PWG1	BiBi	9.2	1	+
PHQMD	PWG2	BiBi	8.8	15	+
			9.2	61	+
			2.4/3.0/4.5	10/10/2	-
vHLLE-UrQMD	PWG3	BiBi	11.5	15	+
		AuAu	11.5	15	+
		AuAu	7.7	20	+
Smash	PWG1	BiBi	9.46	10	+
		ArAr	4/7/9/11	20/20/20/20	-
		AuAu	4/7/9/11	20/20/20/22	-
		XeXe	4/7/9/11	20/20/20/20	-
		CC	4/7/9/11	20/20/20/20	-
		pp	4/7/9/11	50/50/50/50	-
JAM	PWG3	AuAu	3/3.3/3.5/3.8/4.0/4.2/4.5/5	40/40/40/40/40/40/40/40	
DCM-QGSM-SMM	PWG3	AuAu	4/9.2	5/5	+
		AgAg	4/9.2	5/5	+
		BiBi	4/9.2	5/6	+
PHSD		BiBi	9/9.2	25	+
Total				1233(50 underway)	389(50 underway)

MPD data mass production

MC events
> 1300M

Reconstructed events
> 500M

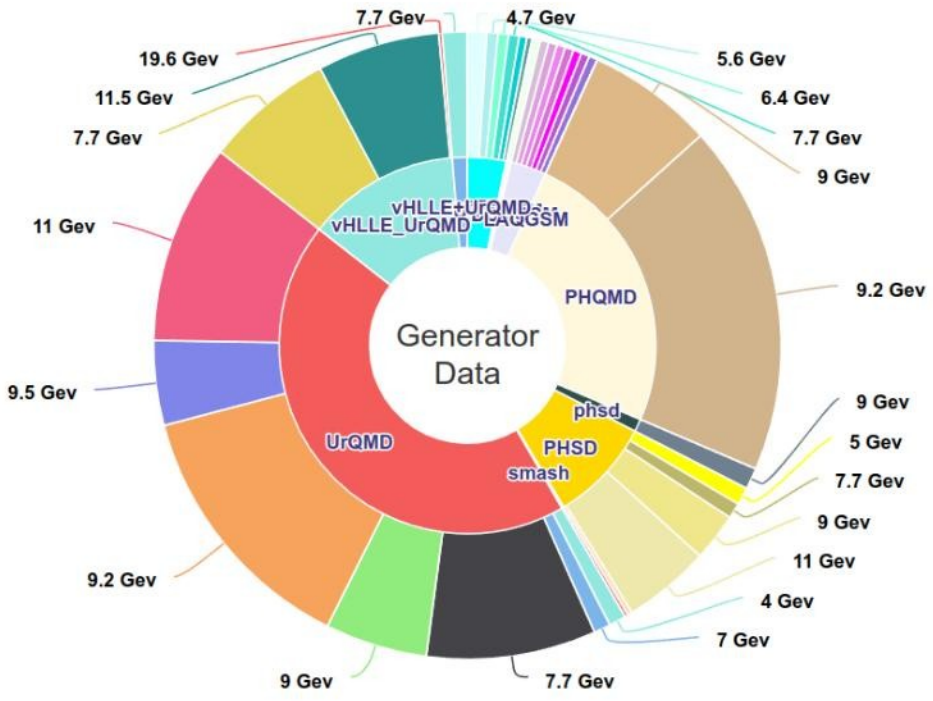

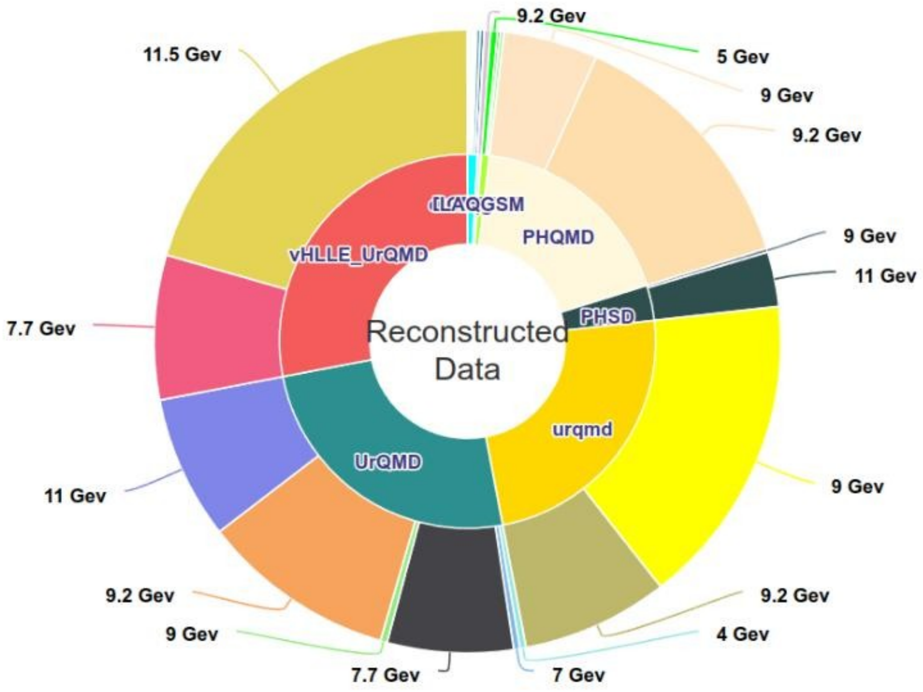

Computing resources for MPD

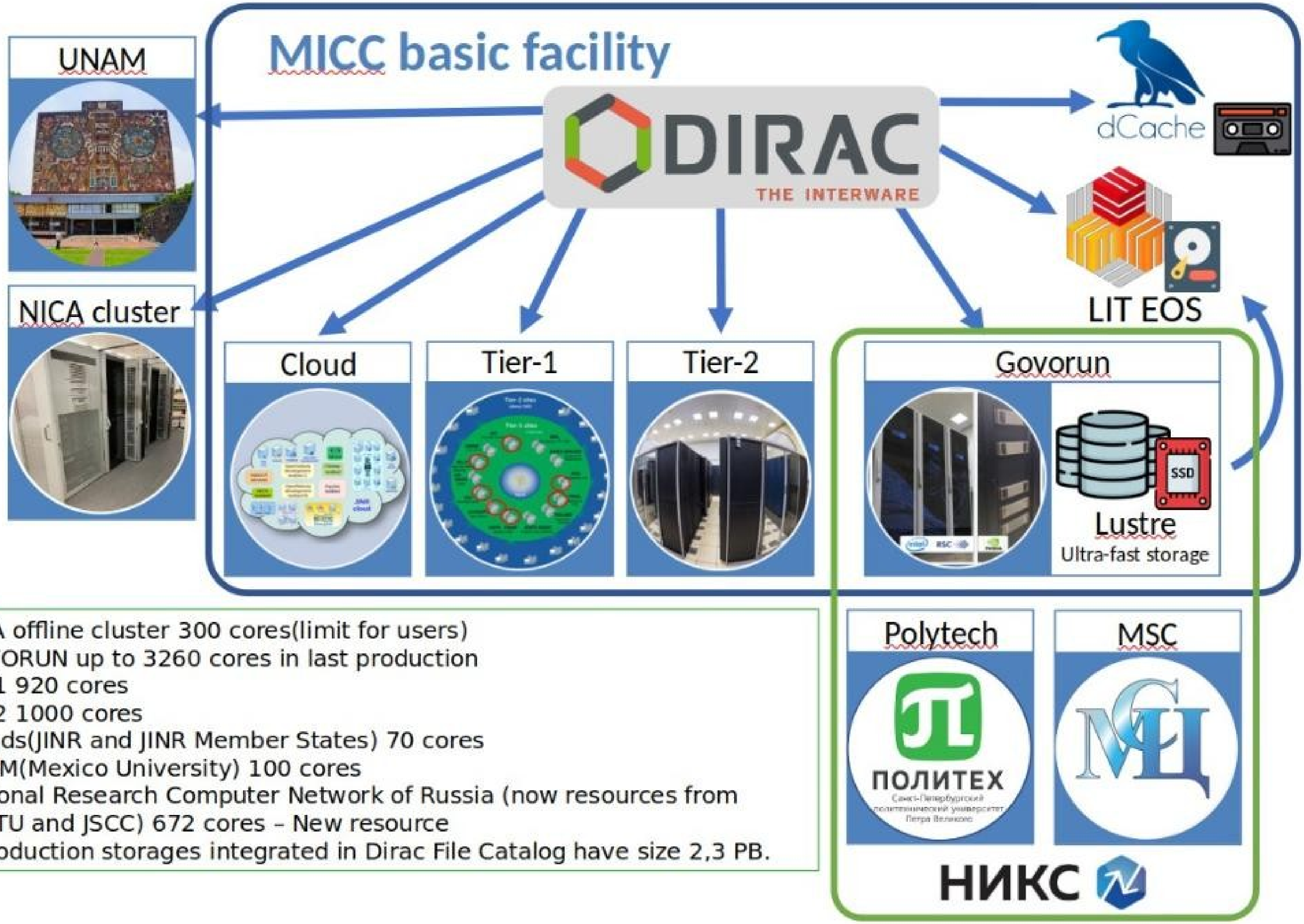

- NICA offline cluster 300 cores(limit for users)
- GOVORUN up to 3260 cores in last production
- Tier1 920 cores
- Tier2 1000 cores
- Clouds(JINR and JINR Member States) 70 cores
- UNAM(Mexico University) 100 cores
- National Research Computer Network of Russia (now resources from SPBTU and JSCC) 672 cores – New resource

Mass production storages integrated in Dirac File Catalog have size 2,3 PB.

Software frameworks for NICA experiments

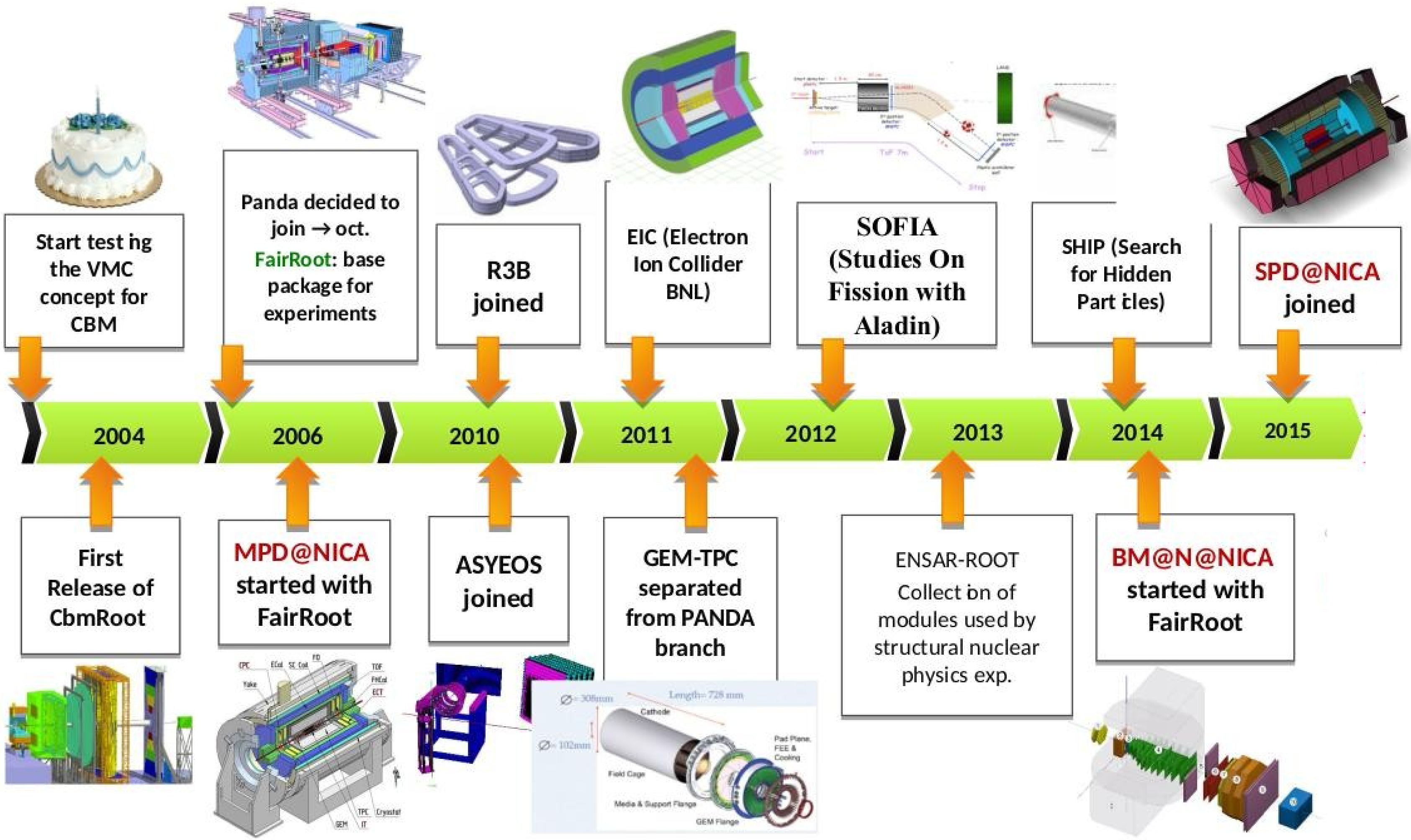

MPD physics

Global observables

- Total event multiplicity
- Total event energy
- Centrality determination
- Total cross-section measurement
- Event plane measurement at all rapidities
- Spectators measurement

Spectra of light flavor and Hypernuclei

- Light flavor spectra
- Hyperons and hypernuclei
- Total particle yields and yield ratios
- Kinematic and chemical properties of the event
- Mapping QCD Phase Diag.

Correlations and Fluctuations

- Collective flow for hadrons
- Vorticity, Λ polarization
- E-by-E fluctuation of multiplicity, momentum and conserved quantities
- Femtoscopy
- Forward-Backward corr.
- Jet-like correlations

Electromagnetic probes

- Electromagnetic calorimeter meas.
- Photons in ECAL and central barrel
- Low mass dilepton spectra in-medium modification of resonances and intermediate mass region

Heavy flavor

- Study of open charm production
- Charmonium with ECAL and central barrel
- Charmed meson through secondary vertices in ITS and HF particles
- Explore production at charm threshold

MPD PW1 studies

Event plane resolution

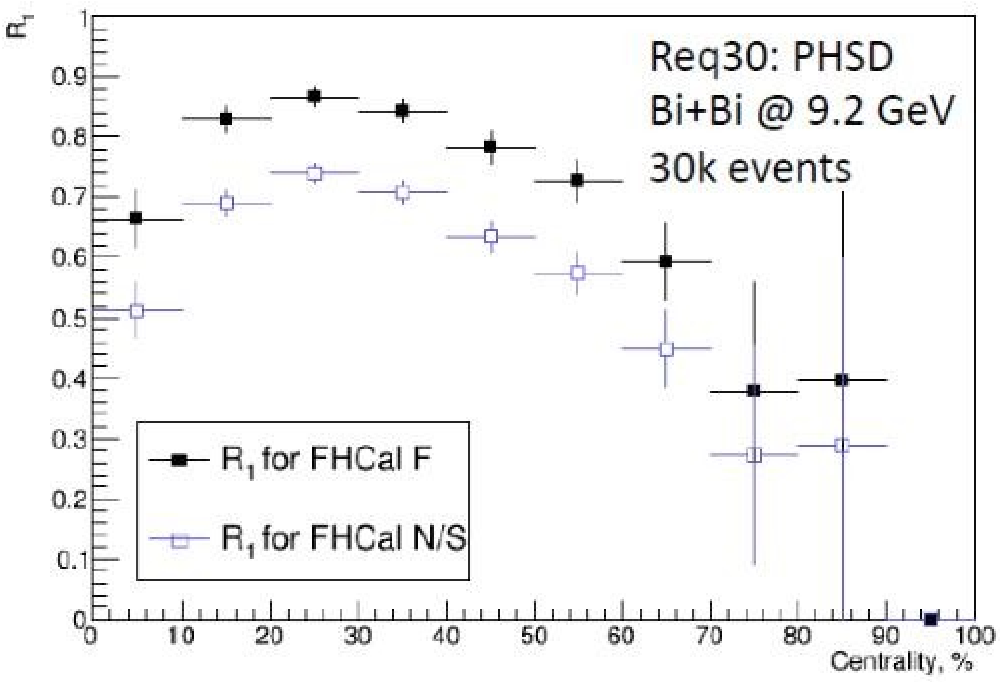

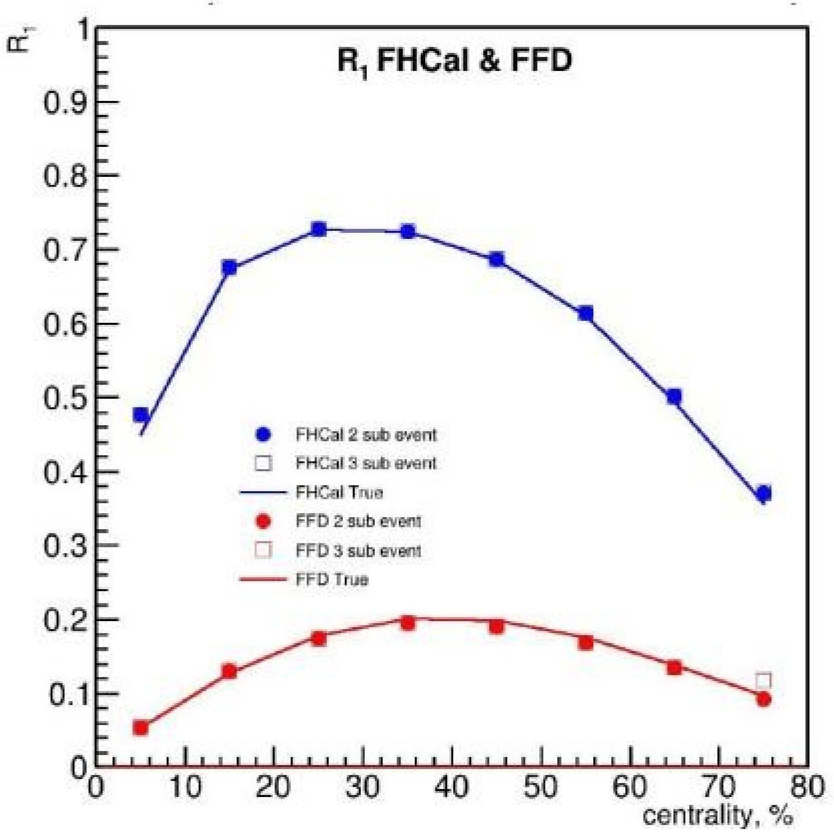

MPD PW1 studies

Event plane resolution

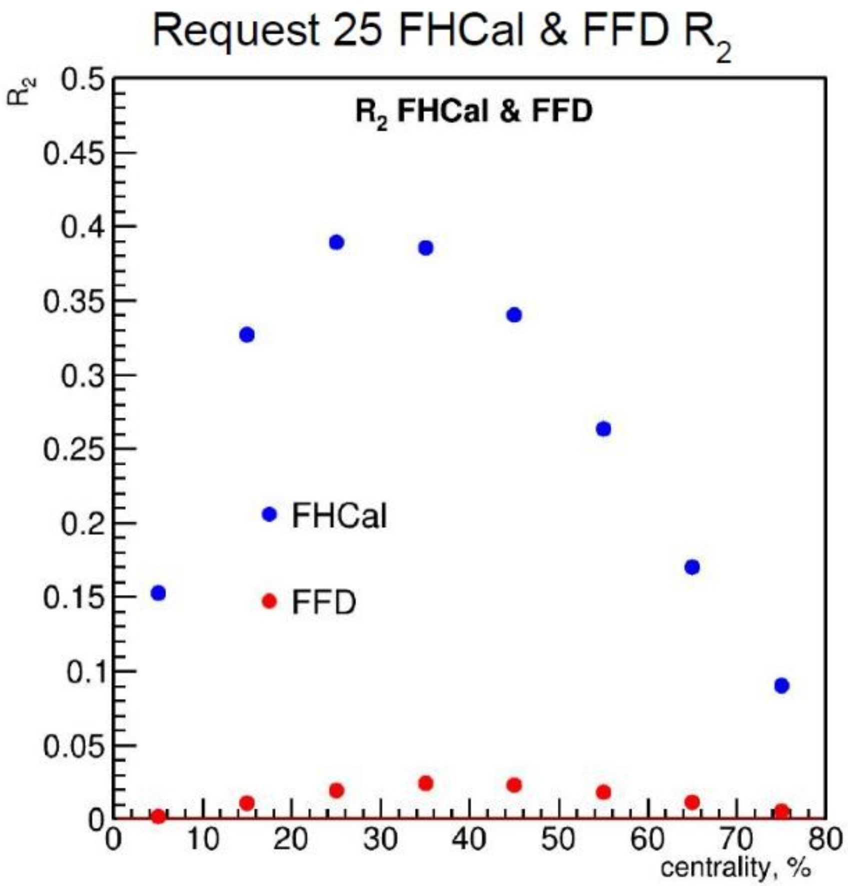

2 sub event $$R_{1,i} = \sqrt{\langle Q^N_{1,i} Q^S_{1,i} \rangle}, i = x, y$$

$$R^{True}_{1,i} = \langle Q_{1,i} \Psi_{RP} \rangle$$

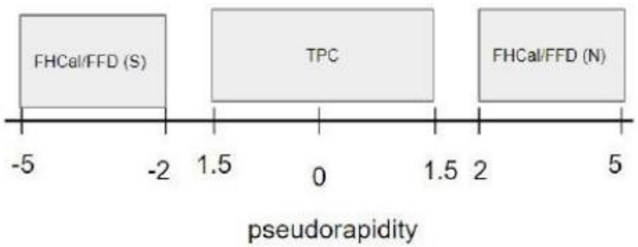

3 sub event $$R^N_{1,i} = \sqrt{\frac{2\langle Q^N_{1,i} Q^S_{1,i} \rangle \langle Q^S_{1,i} Q^{TPC}_{1,i} \rangle}{\langle Q^N_{1,i} Q^{TPC}_{1,i} \rangle}}$$

- FFD resolution are smaller than FHCal
- 2 and 3 sub event has good agreement with True Resolution

MPD PW2 studies

Hyperons in Bi+Bi at 9.2 GeV: no-PID mode at high p_T

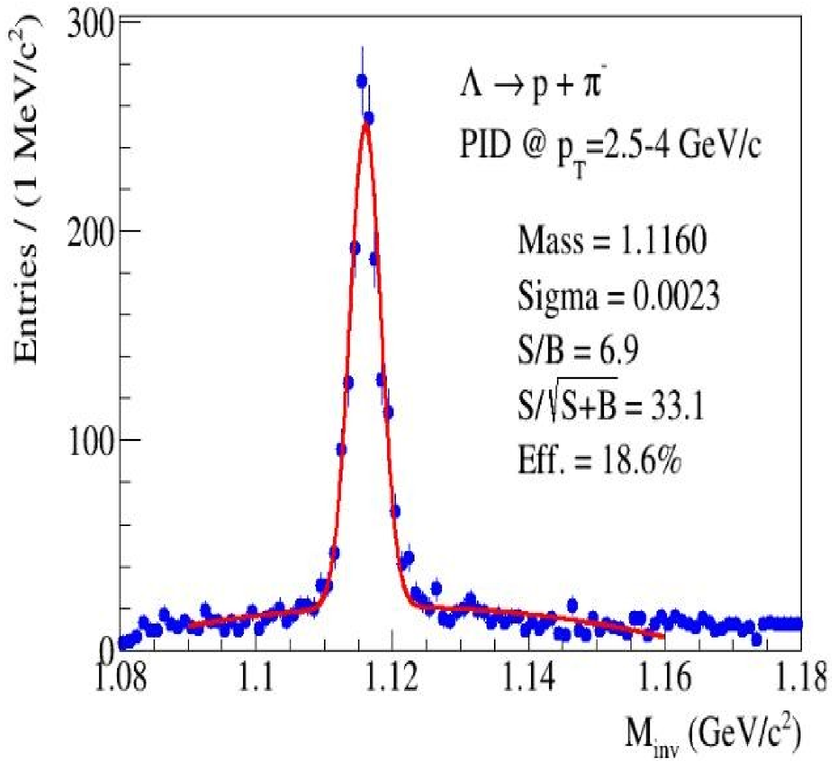

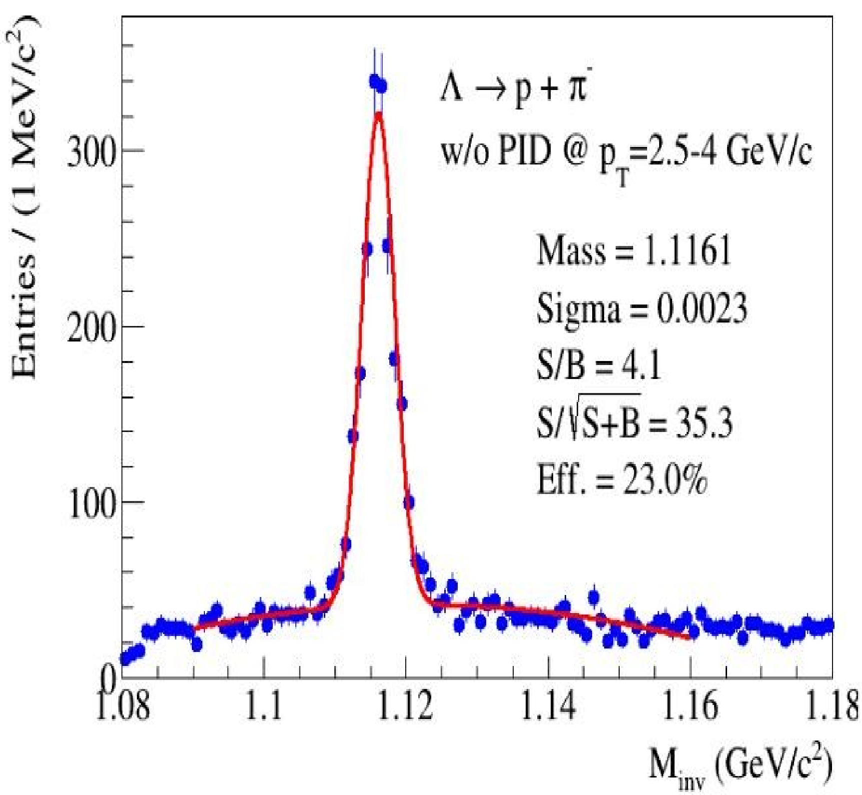

MPD PW2 studies

Global hyperon polarization
at MPD

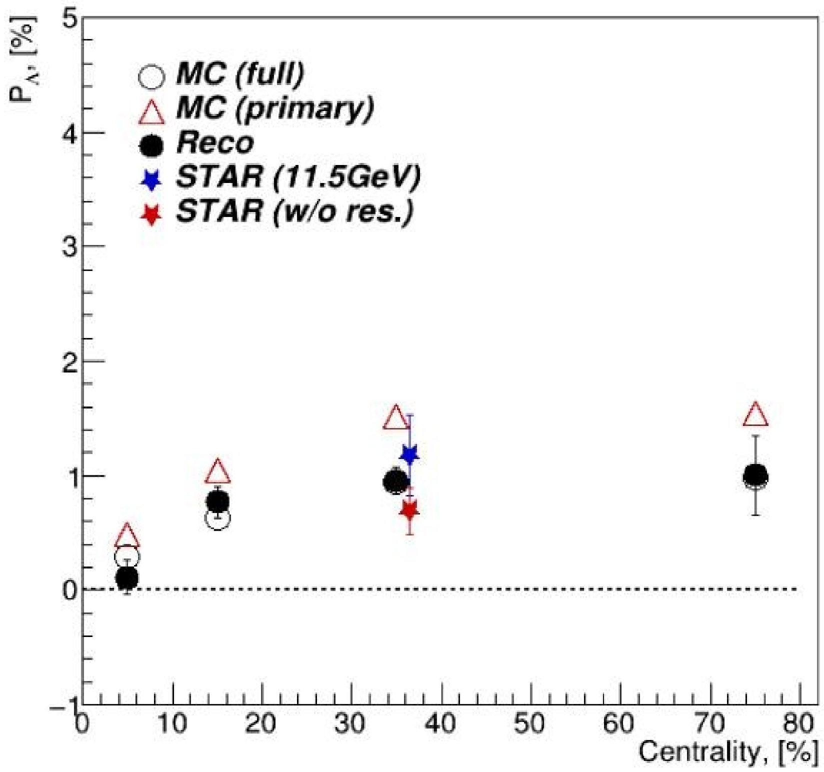

$_{\Lambda}^{3}H$ reconstruction (2-prong)

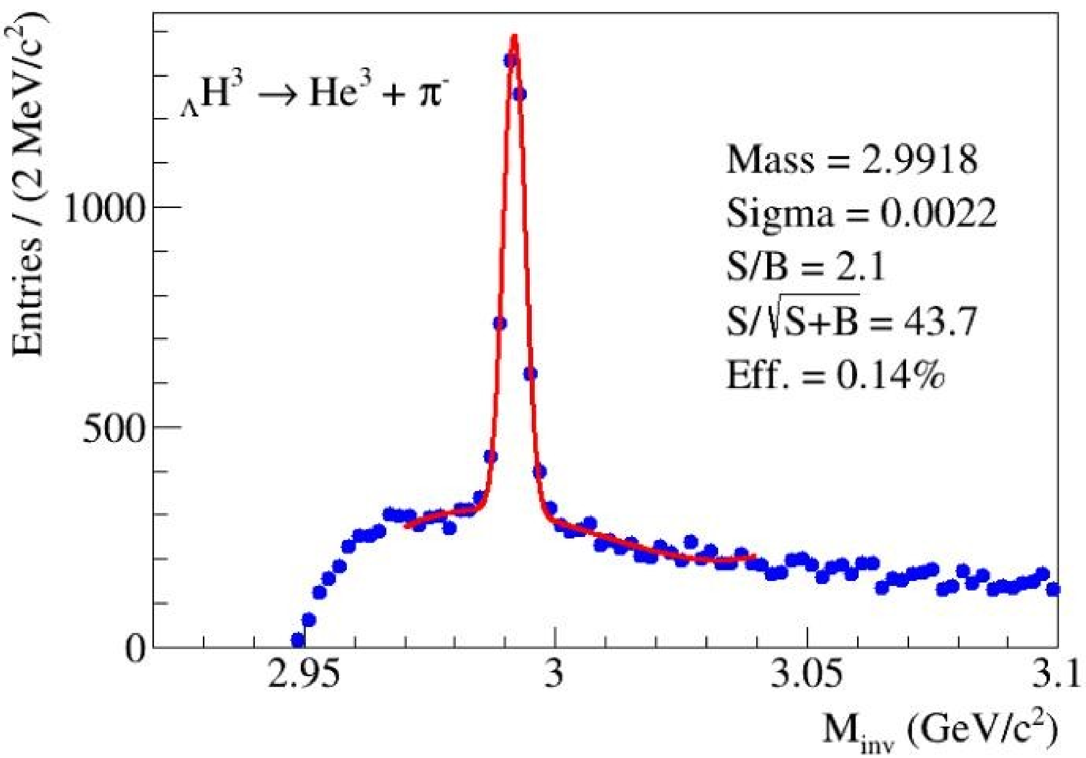

MPD PW3 studies

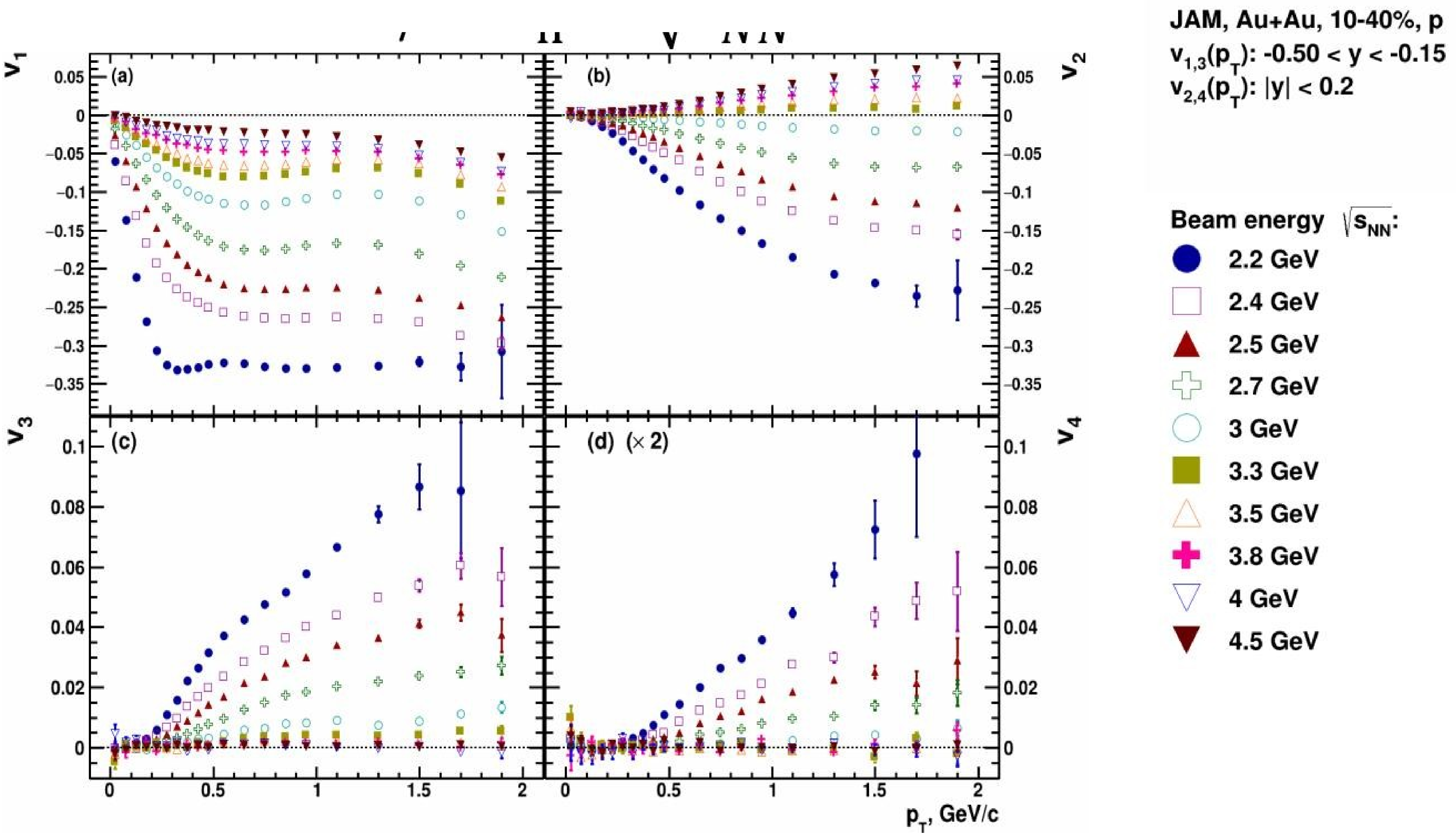

MPD PW3 studies

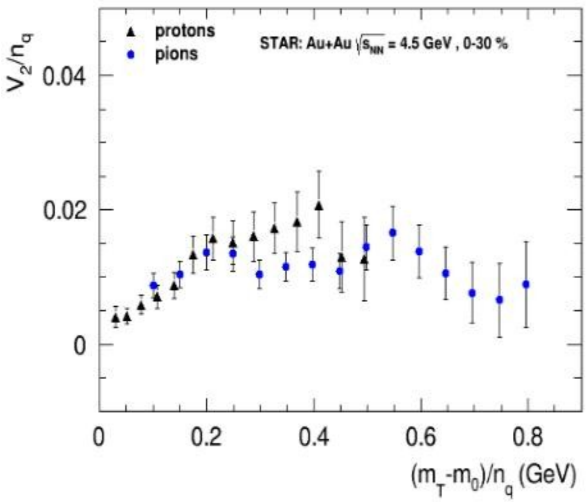

- Scaling holds up at 4.5 GeV in STAR data and pure string/hadronic cascade models (without partonic d.o.f.)

KE_T/n_q scaling at 4.5 GeV might be accidental – more careful studies should be performed

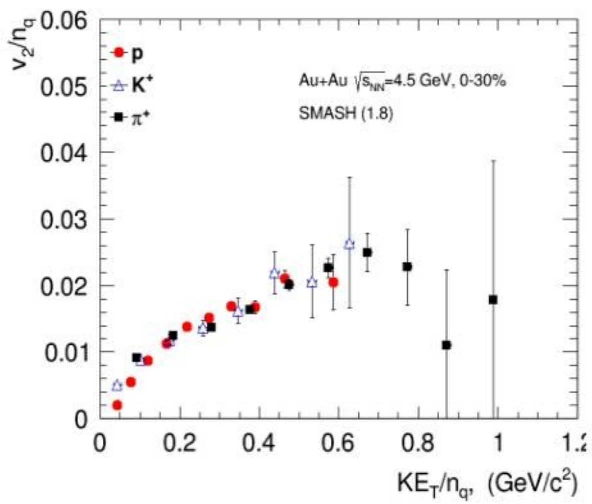

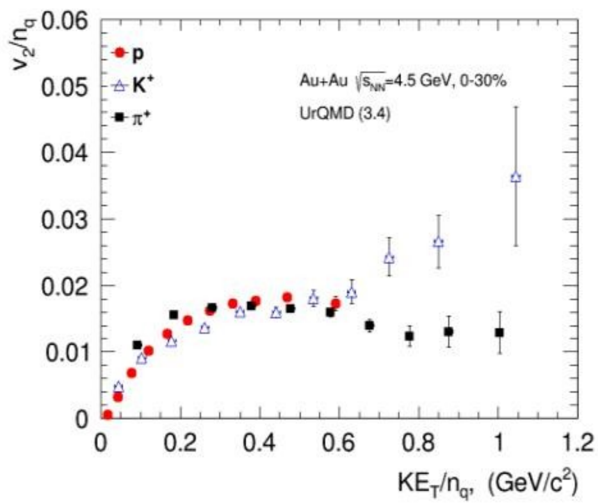

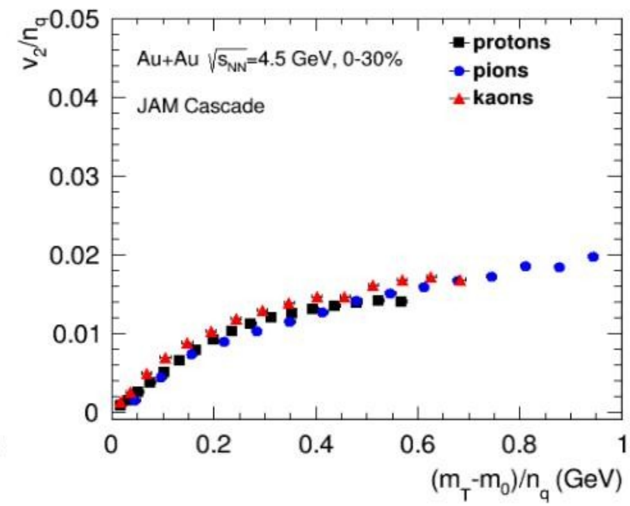

MPD PW4 studies

electromagnetic probes

- ✓ electromagnetic calorimeter (ECAL) reconstruction software
- ✓ reconstruction of photons and neutral meson
- ✓ dielectron continuum and LVMs
- ✓ estimation of direct photon yields and flow

Analyses in the pipeline:

- ✓ $\pi^0/\eta \to \gamma\gamma$, $\pi^0/\eta \to \gamma(e^+e^-)$, $\pi^0/\eta \to (e^+e^-)(e^+e^-)$
- ✓ $K_s \to \pi^0\pi^0$
- ✓ $\omega \to \pi^0\gamma$, $\omega/\eta \to \pi^0\pi^+\pi$
- ✓ $\eta' \to \eta\pi^+\pi^-$
- ✓ $\Sigma^0 \to \Lambda\gamma$, $\Sigma^0 \to \Lambda(e^+e^-)$, $\Sigma^+ \to p\pi^0$
- ✓ inclusive and direct photons
- ✓ dielectron continuum and LVMs
- ✓ single e_{HF}

MPD PW4 studies

PWG4 scope - electromagnetic probes

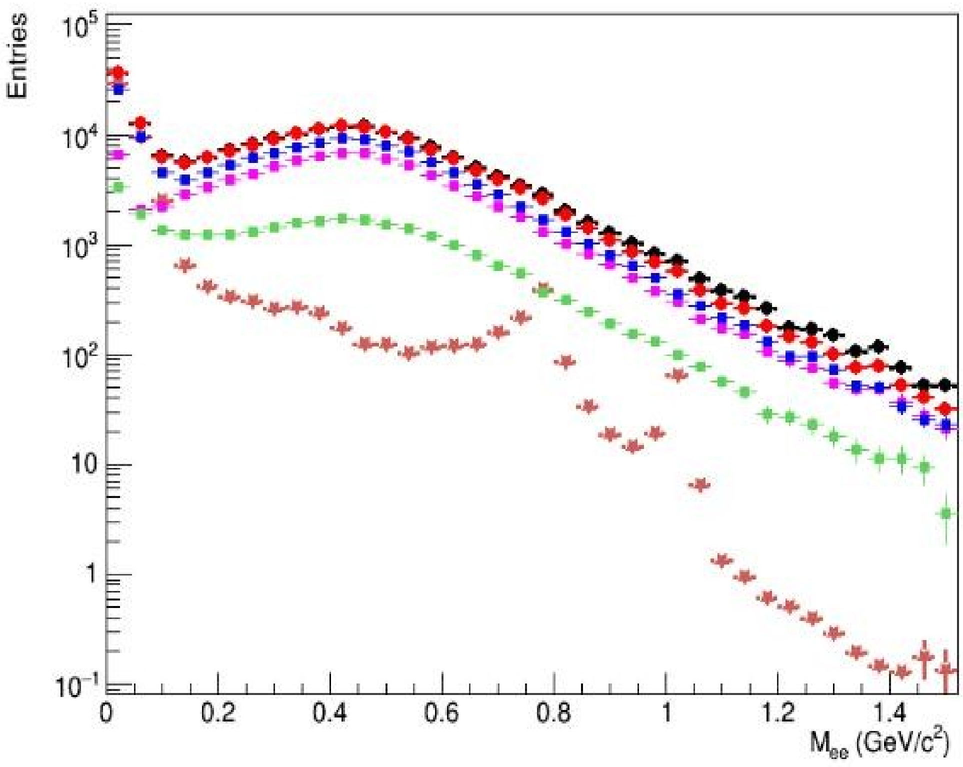

Dielectron continuum (TPC-TOF eID)
Dielectron continuum (perfect eID)
Pairs with π^0 Dalitz electron(s)
Pairs with conversion electron(s)
Pairs with η Dalitz electron(s)
True e^+e^- signal to be measured

BM@N experiment at NICA

setup in experimental run with 3.2 AGeV Ar beam, 2018

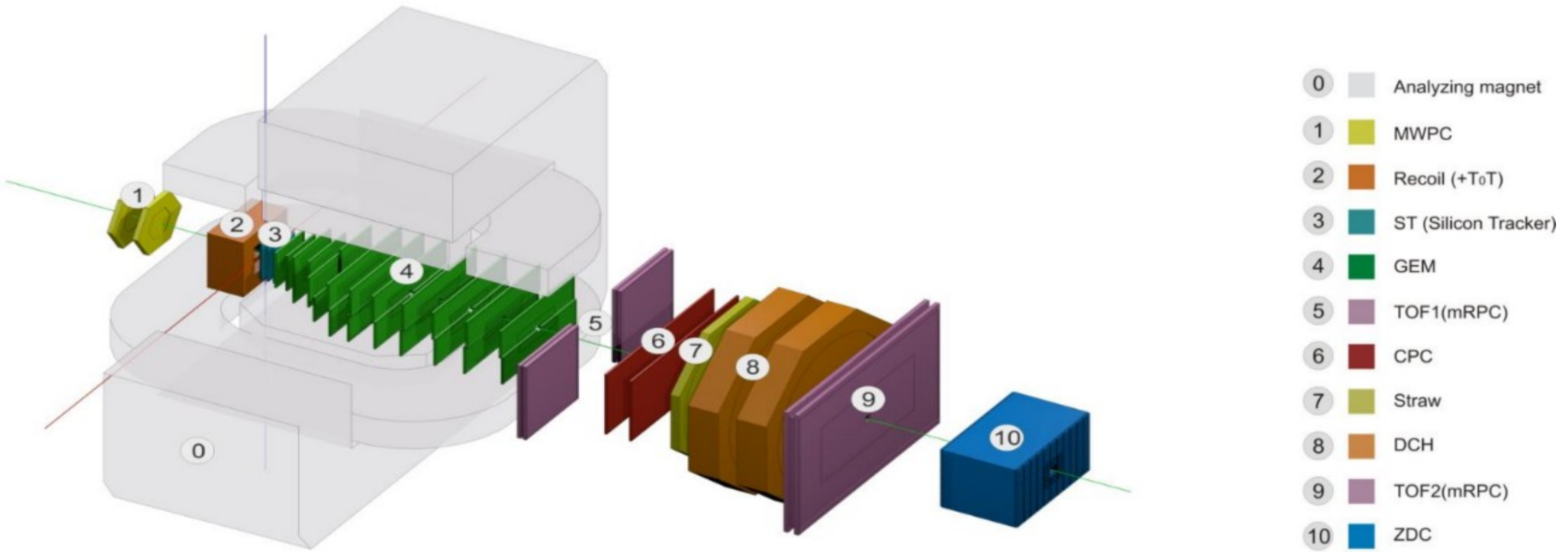

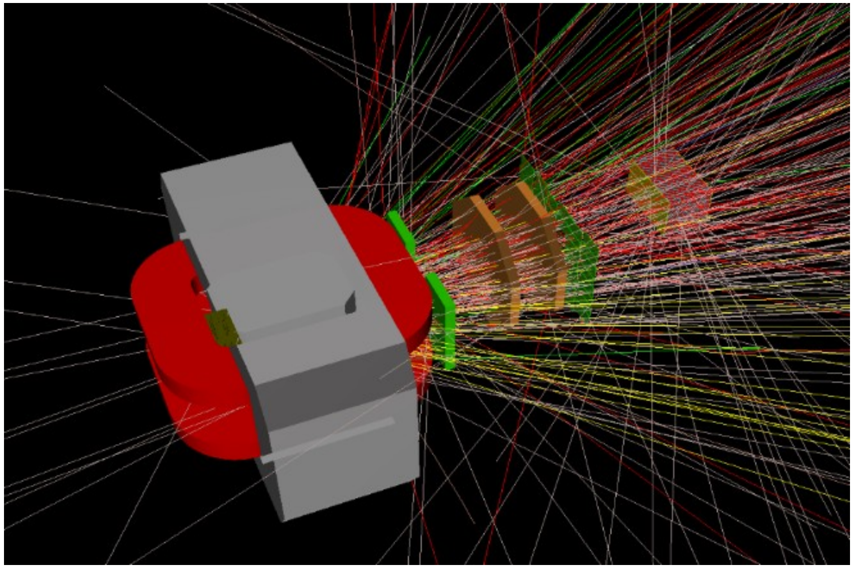

AuAu E_{beam} = 4 GeV

BM@N experiment at NICA

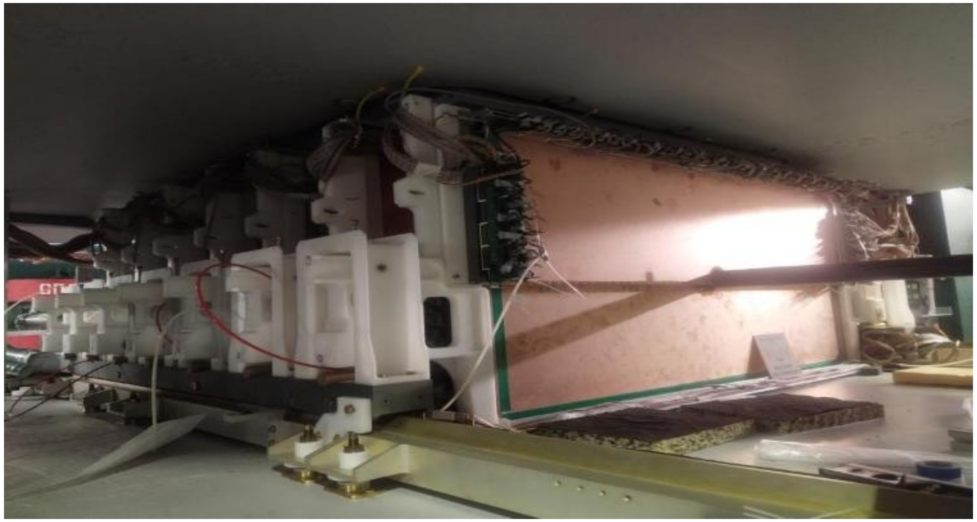

π^+ and K^+ mesons at 3.2 AGeV argon-nucleus collisions

https://arxiv.org/abs/2303.16243v3

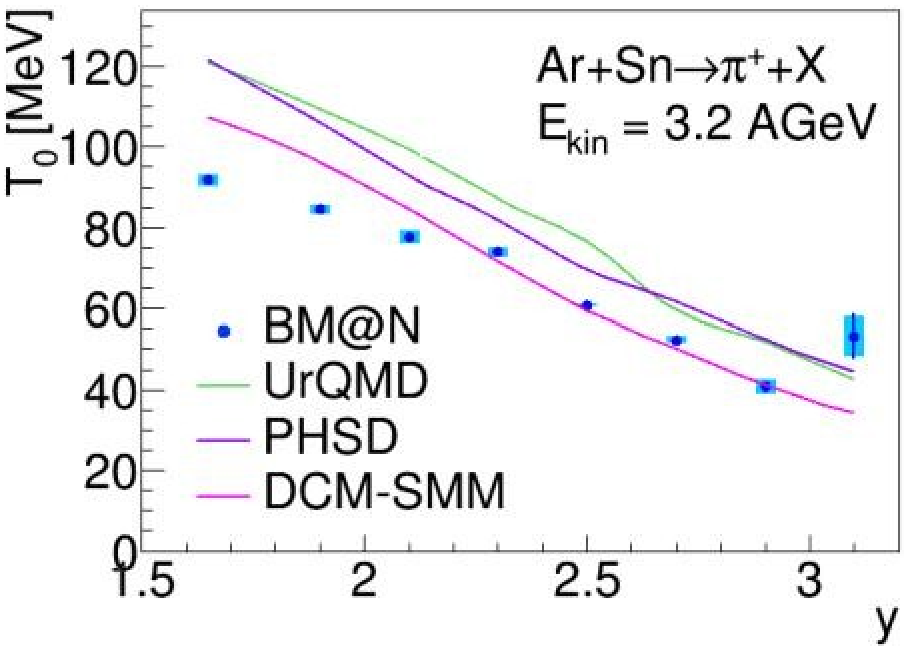

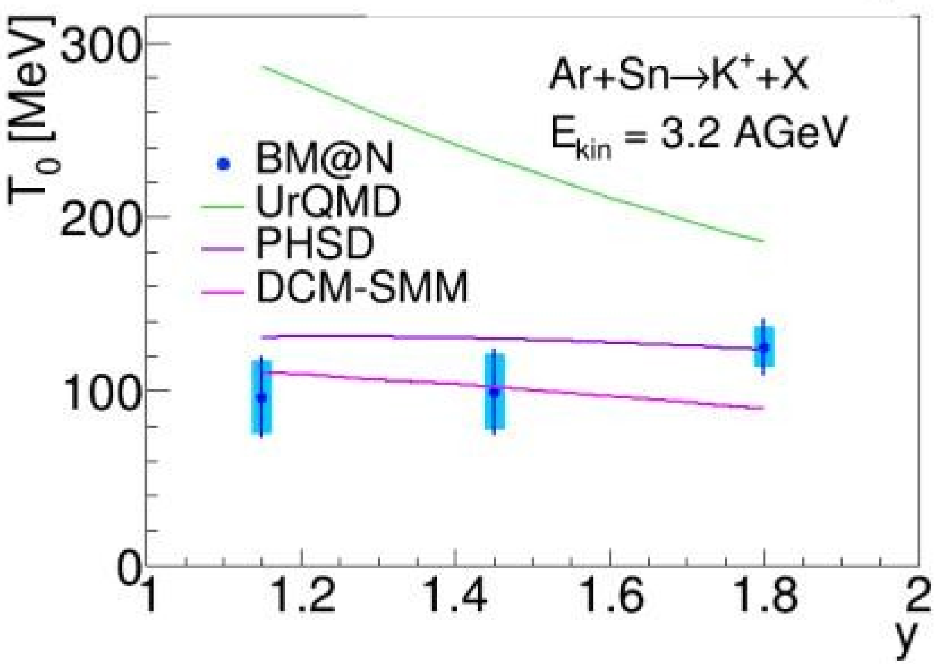

BM@N data (2023 Xe + CsI runs)

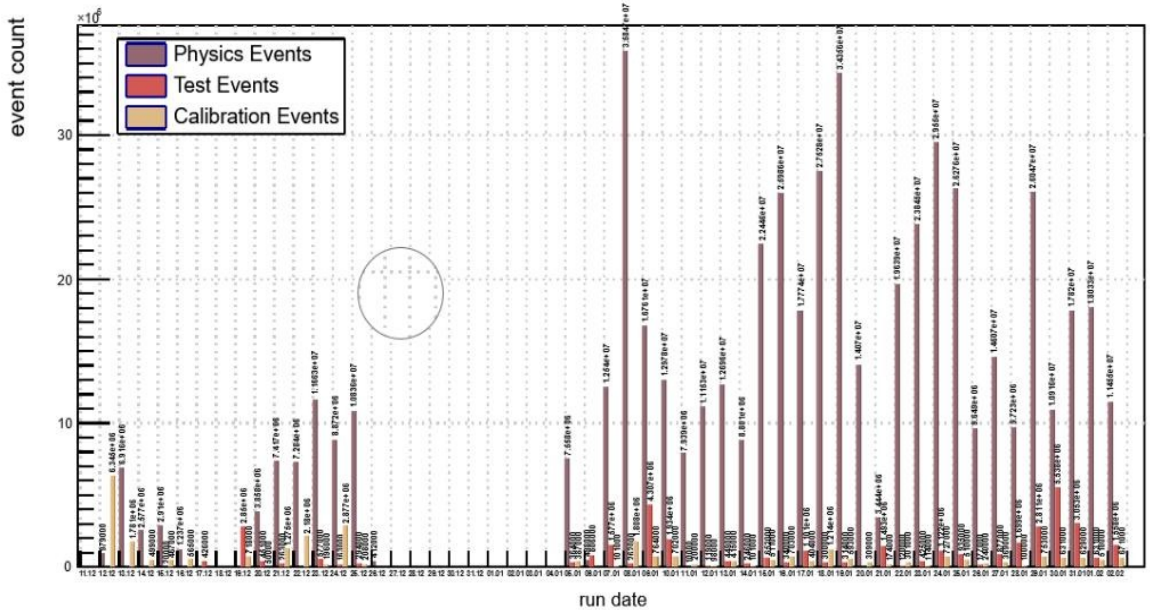

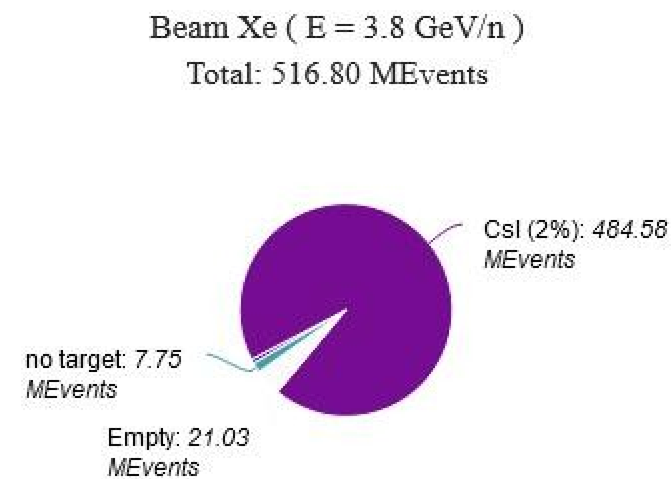

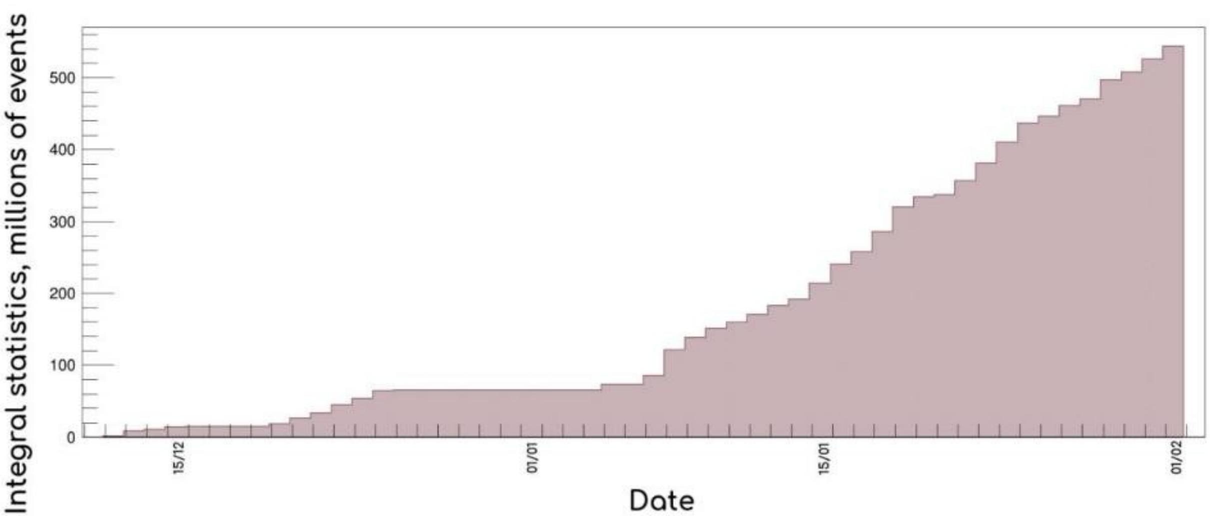

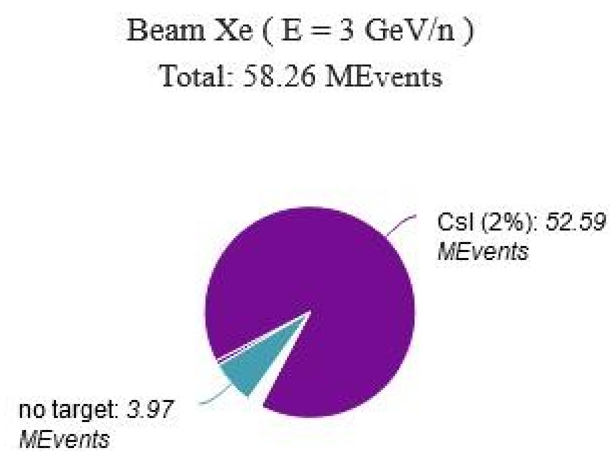

BM@N Λ^0, K_s^0 reconstruction
(2023 Xe + CsI runs)

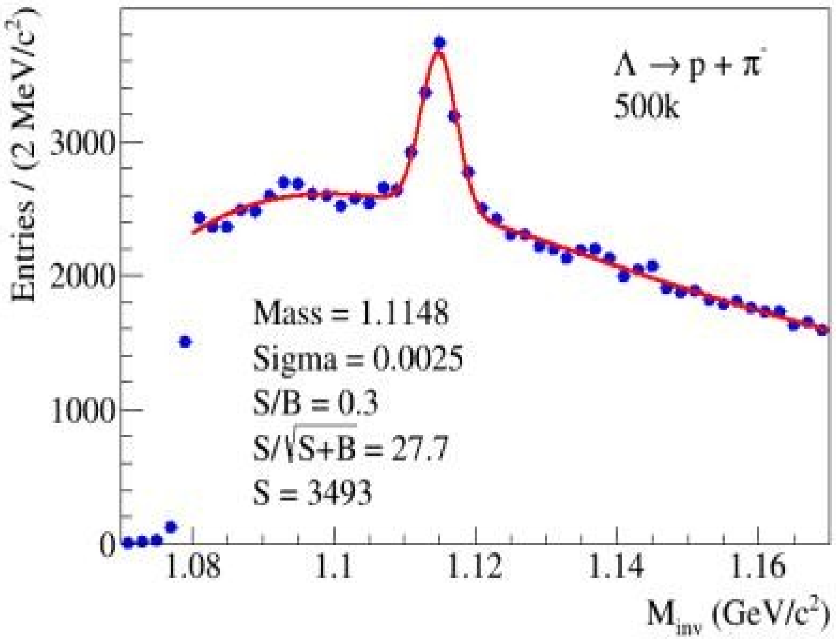

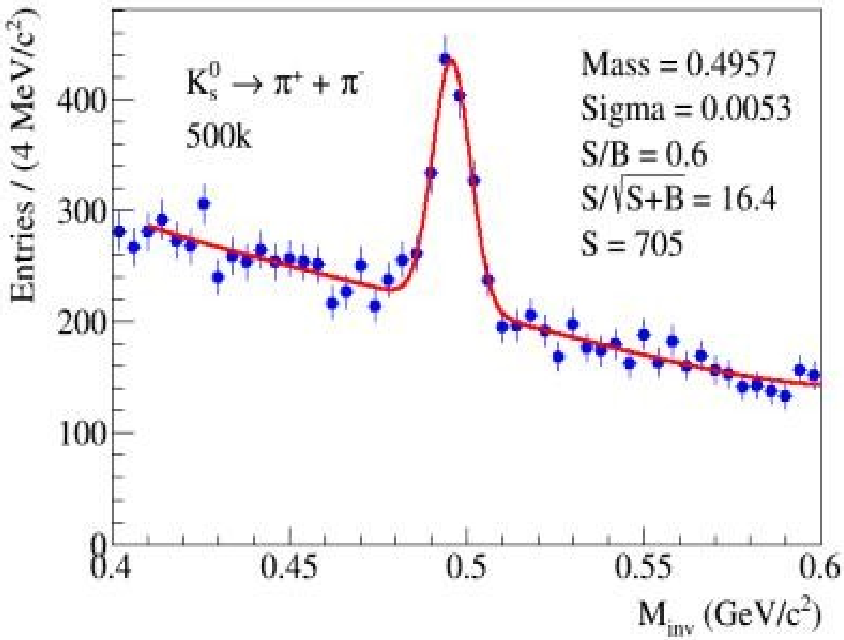

reconstruction efficiency of 2%

BM@N experiment after 2025

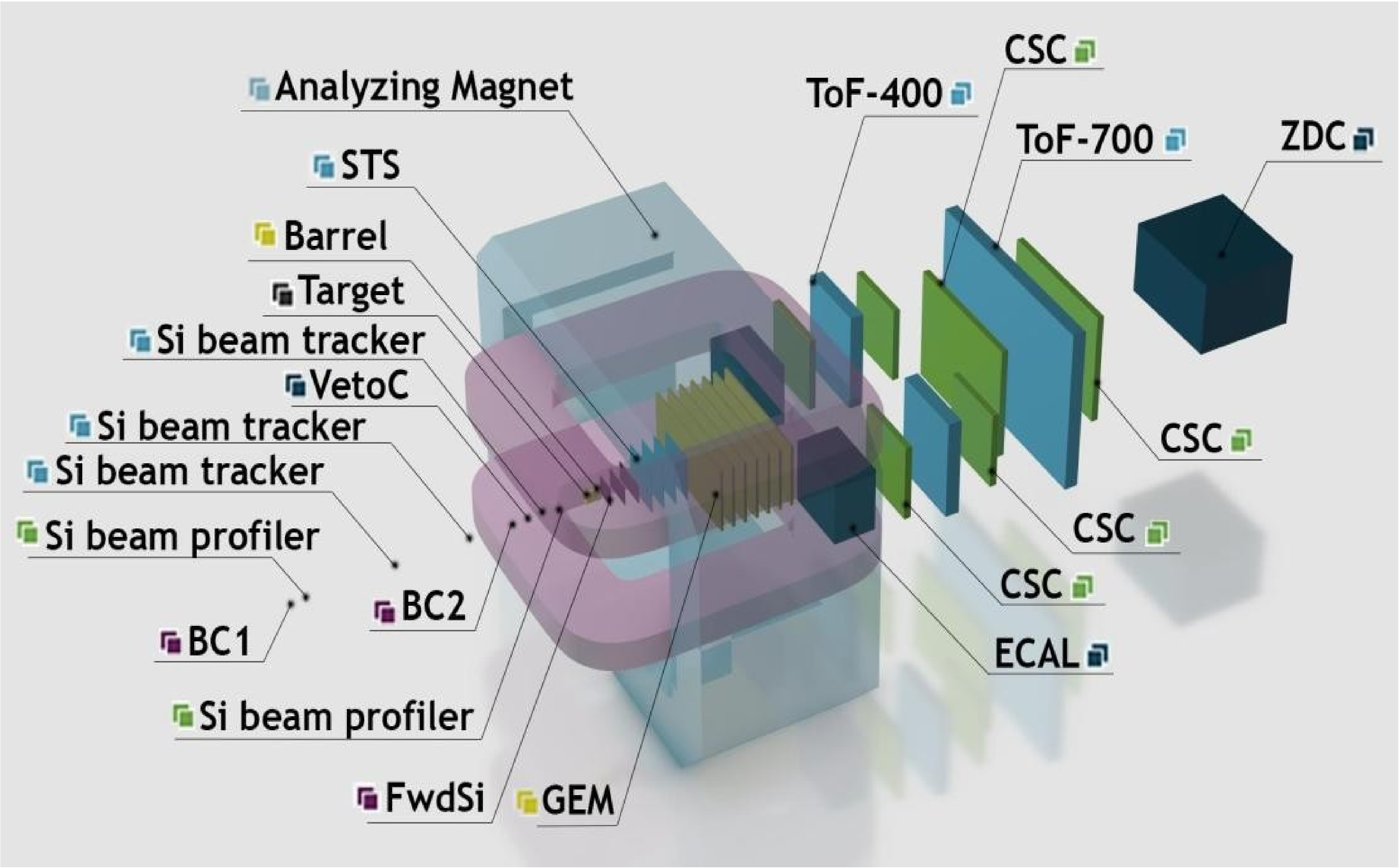

Thank you for attention

to NICA
Relativistic Nuclear Physics

Resent & future experiments for HIC

Facility	SPS	RHIC BES II	Nuclotron M	NICA	SIS/100 (300)	J-PARK HI
Laboratory	CERN Geneva	BNL Brookhaven	JINR Dubna	JINR Dubna	FAIR GSI Darmstadt	J-PARK
Experiment	NA61 SHINE	STAR PHENIX	BM@N	MPD	HADES CBM	JHITS
Start of data taking	2011	2017	2015	2019	2020/25	2025
$\sqrt{s_{NN}}$ (GeV)	4.9 – 17.3	7.7 – 200	< 3.5	4 - 11	2.7 – 8.2	2.0 – 6.2
Physics	CP & OD	CP & OD	HDM	OD & HDM	OD & CP	OD& HDM

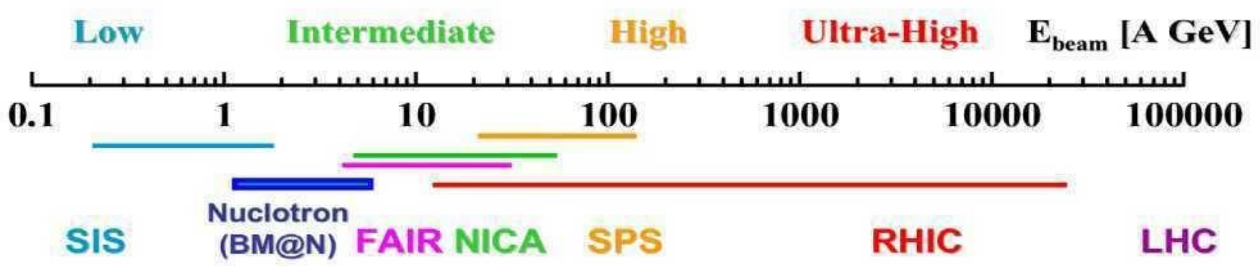

CP — critical point
OD — onset of deconfinement, mixed phase, 1st order phase transition
HDM — hadrons in dense matter
PDM — properties of deconfined matter

New State of Matter created at CERN

Geneva, 10 February 2000. At a special seminar on 10 February, spokespersons from the experiments on CERN1's Heavy Ion programme presented compelling evidence for the existence of a new state of matter in which quarks, instead of being bound up into more complex particles such as protons and neutrons, are liberated to roam freely.

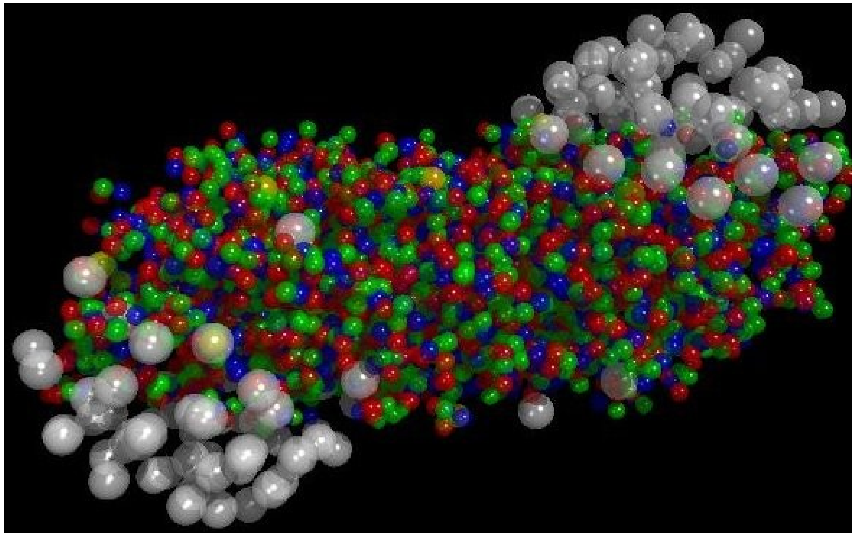

Professor Luciano Maiani, CERN Director General, said "The combined data coming from the seven experiments on CERN's Heavy Ion programme have given a clear picture of a new state of matter. This result verifies an important prediction of the present theory of fundamental forces between quarks. It is also an important step forward in the understanding of the early evolution of the universe. We now have evidence of a new state of matter where quarks and gluons are not confined. There is still an entirely new territory to be explored concerning the physical properties of quark-gluon matter. The challenge now passes to the Relativistic Heavy Ion Collider at the Brookhaven National Laboratory and later to CERN's Large Hadron Collider."

The lead beam programme started in 1994, after the CERN accelerators has been upgraded by a collaboration between CERN and institutes in the Czech Republic, France, India, Italy, Germany, Sweden and Switzerland. A new lead ion source was linked to pre-existing, interconnected accelerators, at CERN, the Proton Synchrotron (PS) and the SPS. The seven large experiments involved measured different aspects of lead-lead and lead-gold collisions. They were named NA44(link is external), NA45(link is external), NA49, NA50, NA52(link is external), WA97 / NA57and WA98. Some of these experiments use multipurpose detectors to measure and correlate several of the more abundant observable phenomena. Others are dedicated experiments to detect rare signatures with high statistics. This co-ordinated effort using several complementing experiments has proven very successful.

QGP in nucleus collisions

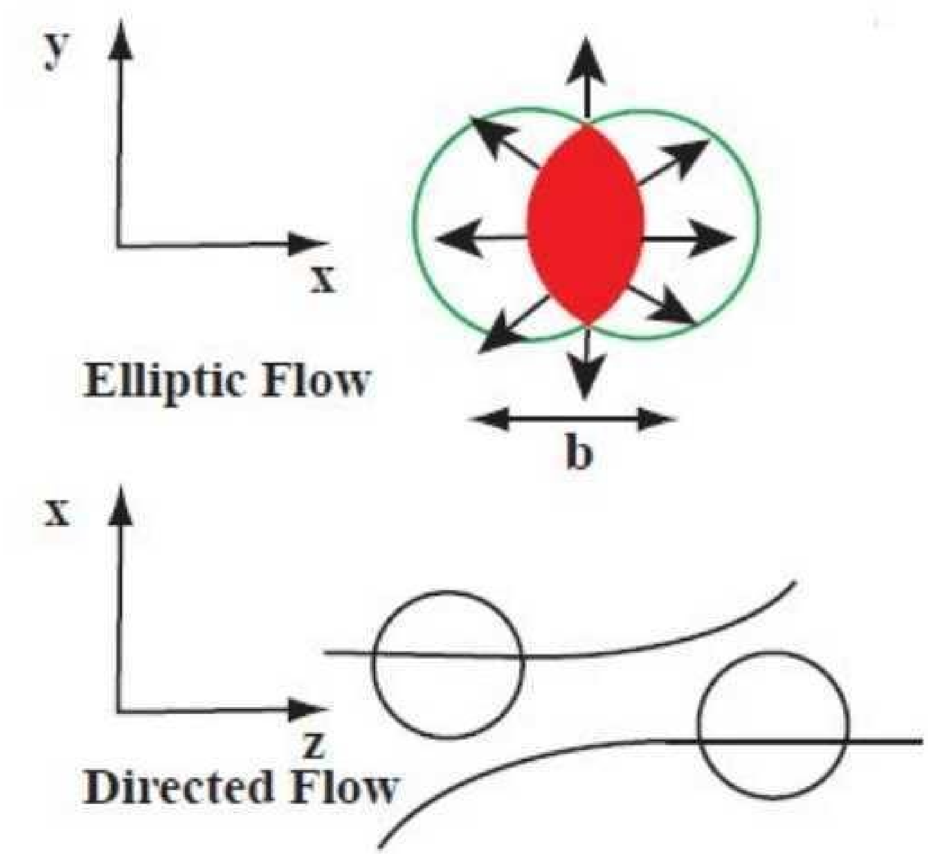

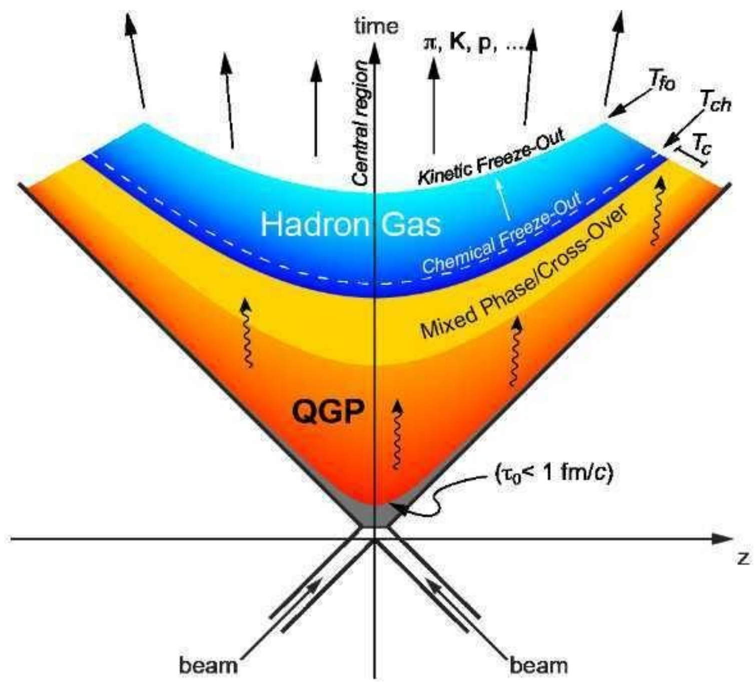

STAR BES I results

High P_T suppression

Stephen Horvat   Quark Matter 2015

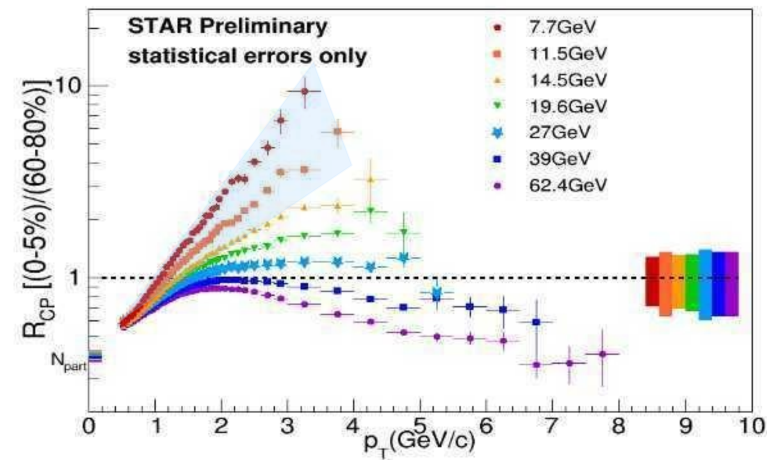

Number of constituent quarks scaling

Phys. Rev. C88, (2013), 014902

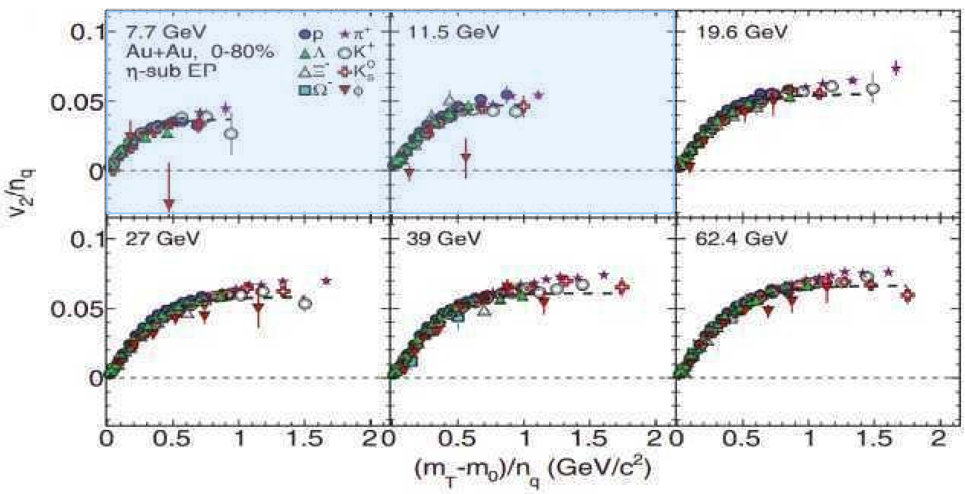

Chiral Magnetic Effect

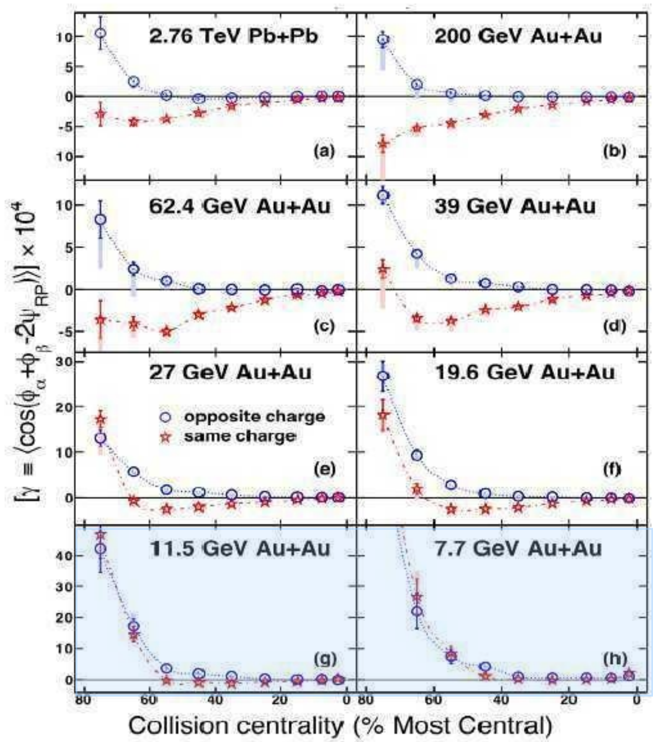

Ridge effect

B. Abelev et al., Phys. Rev. C80, 064912 (2009).

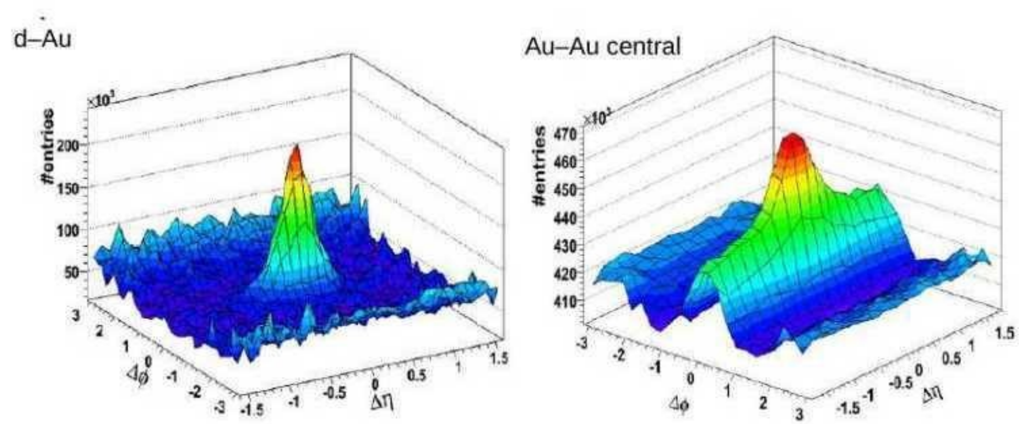

STAR BES I results

PRL 112 (2014) 162301

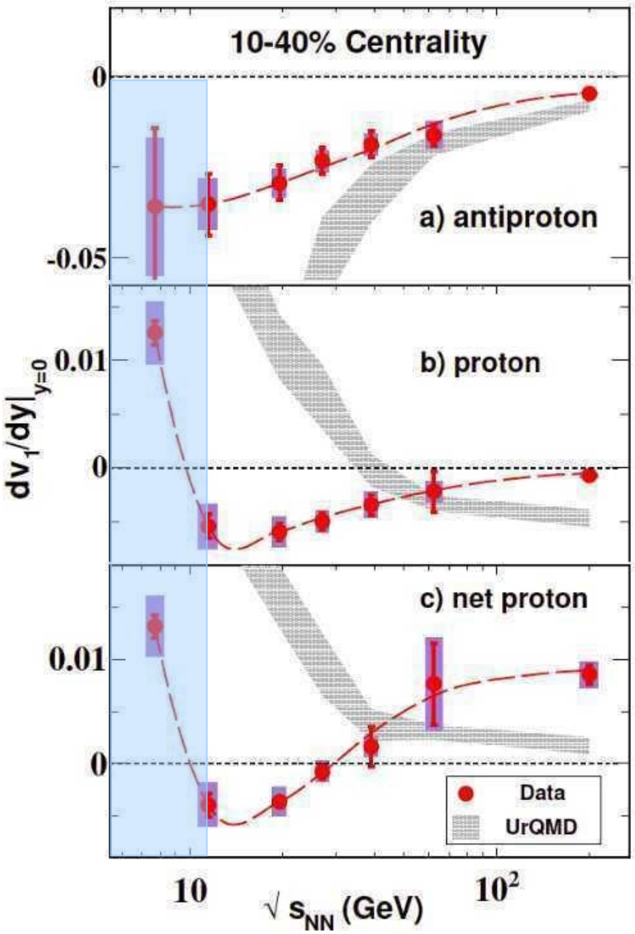

The rapidity-slope of the net proton directed flow v_1, dv_1/dy. This quantity is sensitive to early pressure gradients in the medium.

R. Lacey, PRL 114, 142301 (2015)

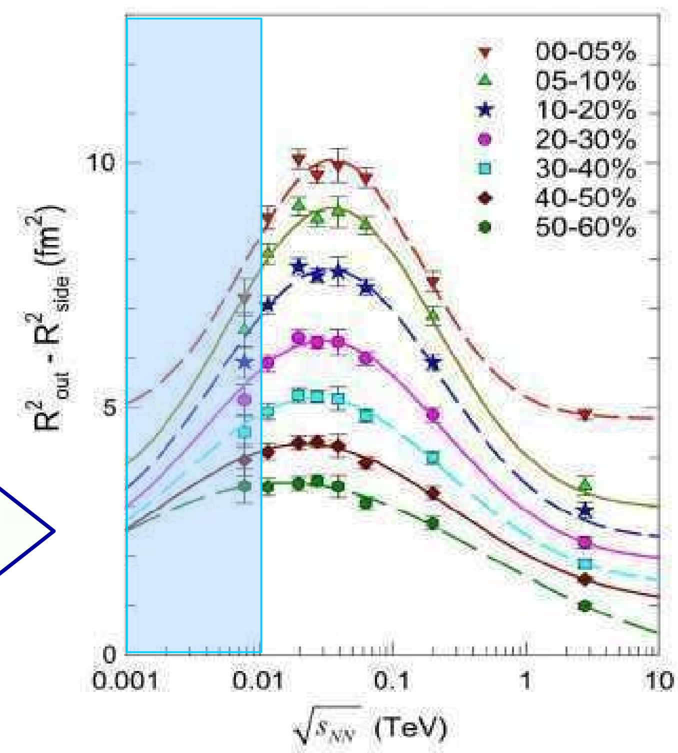

R^2_{out} - R^2_{side} – reflects the lifetime of the collision fireball and was predicted to reach a maximum for collisions in which a hydrodynamic fluid forms at temperatures where the equation of state is softest.

STAR BES I results

STAR, PRL 112, 032302 (2014)

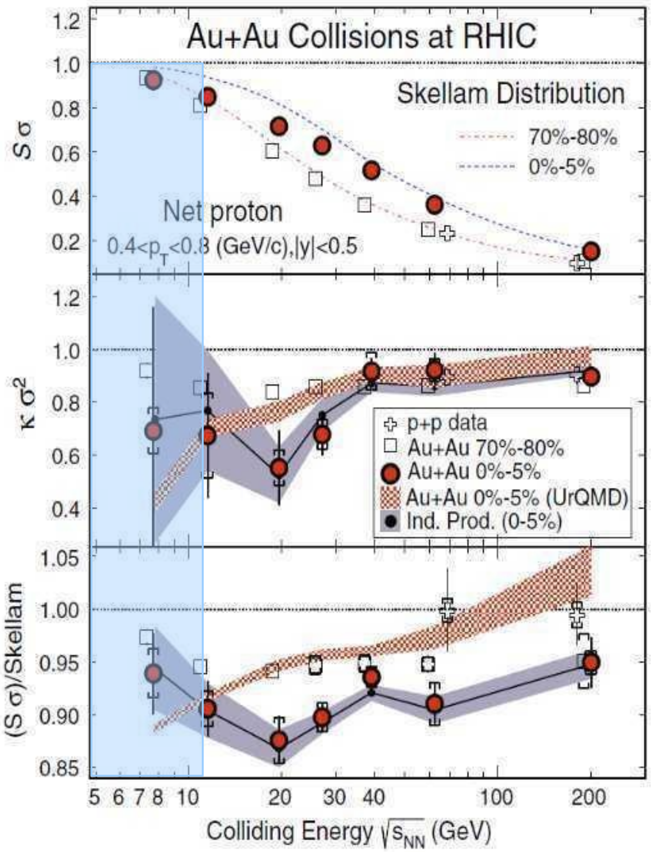

The kurtosis of the event-by-event distribution of the net proton (i.e. proton minus antiproton) number per unit of rapidity, normalized such that Poisson fluctuations give a value of 1.

In central collisions, published results in a limited kinematic range show a drop below the Poisson baseline around $\sqrt{s_{NN}}$ =27 and 19.6 GeV.

New preliminary data over a larger p_T range, although at present still with substantial error bars, hint that the normalized kurtosis may, in fact, rise above 1 at lower $\sqrt{s_{NN}}$, as expected from critical fluctuations..

The grey band shows the much reduced uncertainties anticipated from BES-II in 2018-2019, for the 0-5% most central collisions.